5G Fixed Wireless Access for Bridging the Rural Digital Divide

by

Andrew Lappalainen

A thesis
presented to the University of Waterloo
in fulfillment of the
thesis requirement for the degree of
Master of Applied Science
in
Electrical and Computer Engineering

Waterloo, Ontario, Canada, 2021

Author's Declaration

I hereby declare that I am the sole author of this thesis. This is a true copy of the thesis, including any required final revisions, as accepted by my examiners.

I understand that my thesis may be made electronically available to the public.

Abstract

Despite the ubiquitous level of mobile and fixed broadband (FB) connectivity that exists for many people today, the availability of high quality FB services in rural communities is generally much lower than in urban communities, which has led to a digital divide. At the same time, rural communities in Canada have a high level of 4G LTE coverage and the mobile digital divide between urban and rural communities is much smaller compared to the FB divide. Traditionally, FB and mobile services were offered over separate technologies by different operators, and evolved separately from one another. However, recently, a convergence between mobile and FB has started to emerge via 4G Fixed Wireless Access (FWA), which has made it possible to take advantage of the high level of cellular coverage in rural communities to offer (limited) FB at lower costs than traditional wired FB.

To bridge the digital divide, rural FWA must be able to provide the same end-to-end experience as urban FB. In in this regard, 4G FWA has been inadequate; however, the recent emergence of 5G, which brings new spectrum, a more efficient radio interface, and multi-user massive MIMO, can make a difference. In the first half of this thesis we outline a vision for how 5G could fix the rural connectivity gap by truly enabling FWA in rural regions. We examine new and upcoming improvements to each area of the 5G network architecture and how they can benefit rural users. Despite those advancements, 5G operators will face a number of challenges in planning and operating rural FWA networks. Therefore, we also draw attention to a number of open research challenges that will need to be addressed.

In the latter half of this thesis, we study the planning of a rural 5G multi-user massive MIMO FWA TDD system to offer fixed broadband service to homes. Specifically, we aim to determine the user limit, i.e., the maximum number of homes that can simultaneously receive a target minimum bit rate (MBR) on the downlink (DL) and a target MBR on the uplink (UL) given a set of network resources (e.g., bandwidth, power, antennas) and given a radius. To attain that limit, we must understand how resources should be shared between the DL and UL and how user selection (as well as stream selection since both the base-station (BS) and the homes are multi-antenna), precoding and combining, and power distribution should be performed. To simplify the problem, we use block diagonalization and propose a static user grouping strategy that organizes homes into fixed groups in the DL and UL (we use different groups for the two directions); then we develop a simple process to find the user limit by determining the amount of resources required to give groups the MBRs. We study the impact of group sizes and show that smaller groups use more streams and enable more homes to receive the MBRs when using a 3.5 GHz band. We then show how the user limit at different cell radii is impacted by the system bandwidth,

the number of antennas at the BS and homes, the BS power, and the DL and UL MBRs. Lastly, we offer insight into how the network could be operated for an arbitrary number of homes.

Acknowledgements

First, I wish to thank my supervisor, Catherine Rosenberg, for her guidance and instruction, and for helping me to think about problems like a researcher. I am also thankful to her for the many opportunities to explore different topics early on in my degree, which enabled me to develop a well-rounded perspective on problems. These experiences will surely benefit me in the future.

Thank you to Patrick Mitran and George Shaker for taking the time to review this thesis and provide feedback.

I have been lucky to collaborate with a number of individuals throughout the duration of my degree. Much thanks to Yuhao Zhang, who provided considerable help with the system and channel model in Chapter 3. Working with Abdalla Hussein and Maryam Amini on a survey paper this past year has been an enriching experience. Thank you both for the numerous discussions and for adding fun and variety to my degree. Thank you to Ara Shaverdian for the many coffee breaks, conversations, and opportunities to bounce ideas off one another.

Thank you to my family for always supporting and encouraging me. Special thanks to my sister, Stefanie, who was always happy to share her on-the-ground perspective from the communities up north.

Finally, my biggest thanks goes to my wife, Anna, for always being my greatest supporter, encouraging me to pursue my passions, reminding me about the importance of taking time to have fun, and for the many adventures over the years.

Dedication

To those suffering from the digital divide. My hope is that this research plays some small part in making your future experiences better.

Table of Contents

List of Figures

List of Tables

List of Abbreviations

3GPP	3rd Generation Partnership Project
4G	4th Generation
5G	5th Generation
5GC	5G Core Network
ATSSS	Access Traffic Steering, Switching, and Splitting
AWGN	Additive White Guassian Noise
BD	Block Diagonalization
BS	Base Station
CRTC	Canadian Radio-television and Telecommunications Commission
CSI	Channel State Information
DL	Downlink
DSL	Digital Subscriber Line
eMBB	Enhanced Mobile Broadband
FB	Fixed Broadband
FDD	Frequency Division Duplex
FWA	Fixed Wireless Access
GWCN	Gateway Core Network
IAB	Integrated Access and Backhaul
IPTV	IP Television
LTE	Long Term Evolution
LOS	Line of Sight

MBR	Minimum Bit Rate
MCS	Modulation and Coding Scheme
MEC	Multi-access Edge Computing
MIMO	Multiple Input Multiple Output
MINLP	Mixed Integer Nonlinear Program
MU-MIMO	Multi-User MIMO
MNO	Mobile Network Operator
MOCN	Multi-Operator Core Network
MORAN	Multi-Operator Radio Acecss Network
MP-TCP	Multipath TCP
mMTC	Massive Machine-Type Communications
MWP2P	Microwave Point-to-Point
N3IWF	Non-3GPP Interworking Function
NFV	Network Function Virtualization
NLOS	Non-Line of Sight
NLP	Nonlinear Program
NR	New Radio
OFDM	Orthogonal Frequency Division Multiplexing
OFDMA	Orthogonal Frequency Division Multiple Access
PD	Power Distribution
PRB	Physical Resource Block
RAN	Radio Access Network
RMa	Rural Macro
RRM	Radio Resource Management
SE	Spectral Efficiency
SINR	Signal to Interference plus Noise Ratio
SVD	Singular Value Decomposition
TDD	Time Division Duplex

UL	Uplink
UE	User Equipment
UPA	Uniform Planar Array
URLLC	Ultra-Reliable Low-Latency Communications
US	User Selection
WFQ	Weighted Fair Queueing
WSR	Weighted Sum Rate
ZF	Zero-Forcing

List of Symbols

B	System bandwidth
B_C	Subchannel bandwidth
C	Number of subchannels
$\mathcal{C}_d(\hat{\mathcal{U}})$	Set of subchannels allocated to group $\hat{\mathcal{U}}$ on the downlink
$\mathcal{C}_u(\hat{\mathcal{U}})$	Set of subchannels allocated to group $\hat{\mathcal{U}}$ on the uplink
$E^c_{k,l}$	Effective channel of stream l of home k on subchannel c
$\mathbf{G}^c_k$	Channel matrix of home k for subchannel c
$I^{c,t}_{k,l,q}$	Binary variable indicating MCS level q is used for stream l of home k on PRB (c,t)
L	Number of streams
M_{BS}	Number of antennas at the base station
M_{H}	Number of antennas at each home
MBR_d	Minimum bit rate on the downlink
MBR_u	Minimum bit rate on the uplink
N	Maximum number of homes that can be simultaneously selected on the downlink or uplink
$n(\mathcal{V}_d, L)$	Number of subchannels required to provide S_d homes MBR_d in 95% of realizations, given a slot configuration T_u and up to L streams
$n(\mathcal{V}_u, L)$	Number of subchannels required to provide S_u homes MBR_u in 95% of realizations, given a slot configuration T_u and up to L streams
$P^{c,t}_{k,l}$	Power allocated to stream l of home k on PRB (c,t)
P_{H}	Power budget at each home

$P_{\max}$	Power budget at the base station
P^d_{PRB}	Power per PRB on the downlink
P^k_{PRB}	Power per PRB on the uplink at home k
$\mathcal{Q}$	Set of pairs (SE_q, S_q) from practical MCS function
$\mathcal{R}$	Cell radius
$r^{c,t}_{k,l}$	Approximate rate given to stream l of home k on PRB (c,t) based on continuous approximation of MCS function
$\bar{r}^{c,t}_{k,l}$	Real rate given to stream l of home k on PRB (c,t) after mapping SINR through practical MCS function
r_{max}	Maximum possible rate given to a user stream on a PRB; equivalent to $B_C SE_{\max}$
$\mathcal{S}$	System setting $(B, C, P_{\max}, P_{\mathrm{H}}, MBR_d, MBR_u, M_{\mathrm{BS}}, M_{\mathrm{H}})$
S_d	Group size on the downlink
S^*_d	Optimal S_d yielding the user limit U^* for a given setting $\mathcal{S}$
S_q	SINR level q of the practical MCS function
S_u	Group size on the uplink
S^*_u	Optimal S_u yielding the user limit U^* for a given setting $\mathcal{S}$
$SE_{\max}$	Maximum spectral efficiency attainable through the practical MCS function
SE_q	Spectral efficiency corresponding to S_q in the practical MCS function
$SINR^{c,t}_{k,l}$	SINR of stream l of home k on PRB (c,t)
$SR_d(U, \mathcal{V}_d)$	Downlink sum-rate when U homes are active and configuration $\mathcal{V}_d$ is used
$SR_u(U, \mathcal{V}_u)$	Uplink sum-rate when U homes are active and configuration $\mathcal{V}_u$ is used
T	Number of slots per frame
T_d	Number of slots allocated to downlink per frame
$\mathcal{T}_d$	Set of downlink slots
T_u	Number of slots allocated to uplink per frame
T^*_u	Optimal T_u yielding the user limit U^* for a given setting $\mathcal{S}$
$\mathcal{T}_u$	Set of uplink slots
U	Total number of homes

U^*	User limit for a given system setting $\mathcal{S}$
$U_d(\mathcal{V}_d, L, C)$	User limit on the downlink for a given downlink configuration $\mathcal{V}_d$, number of streams L, number of subchannels C, and setting $\mathcal{S}$
$U_u(\mathcal{V}_u, L, C)$	User limit on the uplink for a given uplink configuration $\mathcal{V}_u$, number of streams L, number of subchannels C, and setting $\mathcal{S}$
$\hat{\mathcal{U}}$	Static group of homes
$\mathcal{V}$	System configuration (T_u, S_d, S_u)
$\mathcal{V}^*$	Optimal configuration (T_u^*, S_d^*, S_u^*) yielding the user limit U^* for a given setting $\mathcal{S}$
$\mathcal{V}_d$	Downlink configuration (T_u, S_d)
$\mathcal{V}_u$	Uplink configuration (T_u, S_u)
α	Downlink weight used to compute the weighted sum-rate
λ_k	Approximate downlink rate given to home k based on continuous approximation of MCS function
$\bar{\lambda}_k$	Real downlink rate given to home k after mapping SINR of each stream on each PRB through practical MCS function
λ'_k	Approximate uplink rate given to home k based on continuous approximation of MCS function
$\bar{\lambda}'_k$	Real uplink rate given to home k after mapping SINR of each stream on each PRB through practical MCS function
$\omega(U)$	Realization of U homes
$\Omega(U)$	Set of all realizations of U homes

Chapter 1

Introduction

1.1 Overview

Global connectivity is at an all time high, and more users than ever before are participating in the online ecosystem through mobile and fixed broadband (FB) connections. Despite this exciting phenomenon, opportunities to access the online world are not shared equally among the global population. Socioeconomic, political, and geographic factors all play roles in determining the extent to which one can be an online participant [1]. The resultant *digital divide* creates a social disparity between those who have reliable access to online content and can take advantage of all that the Internet has to offer and those who do not and miss out on those opportunities [2].

Even in developed countries such as Canada, the FB experience of rural users continues to lag behind urban users.[1] Figure 1.1 shows the latest data on the availability of different downlink (DL) FB data rates in urban and rural communities in Canada [3]. The availability of high rate FB is sharply divided between urban and rural areas. In 2016, the Government of Canada established a country-wide universal service objective of 50 Mbps in the DL and 10 Mbps in the uplink (UL) with no limits on total data transfer [4], but today less than 50% of Canadians in rural communities are able to access that type of service at home. The issue is even more stark when viewed across Canada's provinces and territories (Table 1.1). In particular, no home in any of Canada's territories is able to

[1]The distinctions between *urban* and *rural* are somewhat subjective. We will follow the definition of rural used by the Canadian Radio-television and Telecommunications Commission (CRTC), which defines rural as communities with populations less than 1000 people or with population densities less than several hundred people per square kilometer [3].

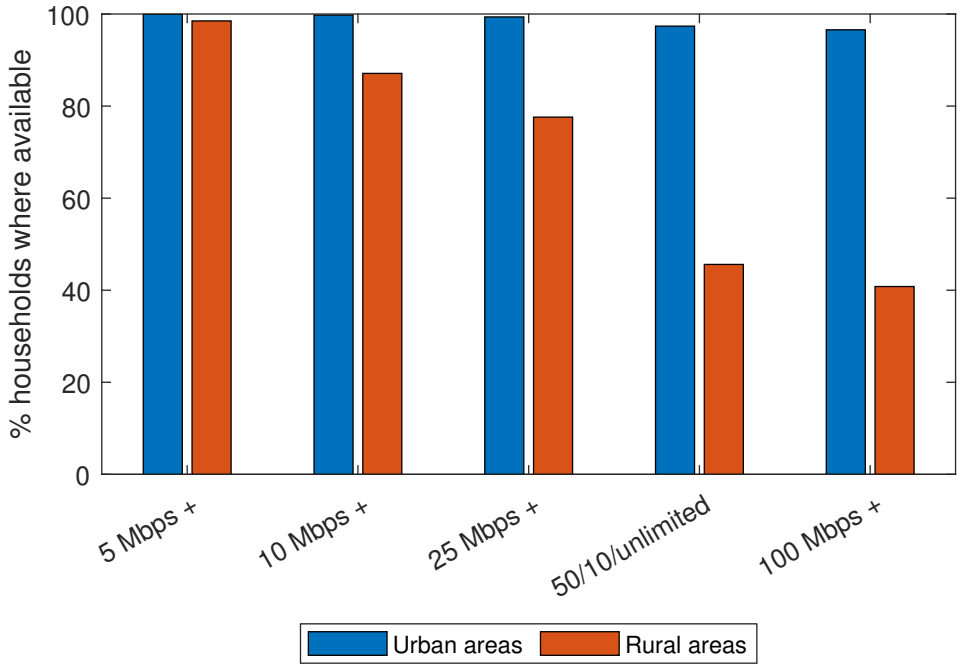

Figure 1.1: Canada fixed broadband availability in 2019 [3]. 50/10/unlimited refers to data rates of 50 Mbps in the downlink and 10 Mbps in the uplink with no limit on the total data transferred. Data for other rates is availabile in the downlink only.

access a connection meeting the universal service objective. Moreover, this data does not reflect the true uptake of a service, but instead the availability of a connection that could provide access to those rates to one willing to pay for the service. Hence, the true number of Canadians failing to meet the universal service standard is even lower than presented.

A key factor for the fixed broadband divide can be attributed to the prohibitive costs to build and operate network infrastructure over large areas relative to the smaller number of users [1]. Hence, the ability to keep rural communities well-connected using traditional wired FB technologies, such as DSL, cable, or fiber, is much costlier on a per-user basis than in urban areas. These heightened costs often translate to network infrastructure that is out-of-date or has under-provisioned capacity. Combined, these factors lead to a degraded quality of experience (QoE) compared to urban communities and limit the extent that

Province/Territory	50/10/unlimited FB availability			LTE availability		
	Urban areas	Rural areas	Difference	Urban areas	Rural areas	Difference
British Columbia	98.6	62.5	36.1	99.9	94.4	5.5
Alberta	97.8	33.2	64.6	99.9	98.9	1
Saskatchewan	96.2	23.9	72.3	99.9	99.4	0.5
Manitoba	93.2	14.4	78.8	99.7	89.1	10.6
Ontario	97.6	30.5	67.1	99.9	98.8	1.1
Quebec	98.3	65.2	33.1	99.9	98.1	1.8
New Brunswick	99.7	63.6	36.1	99.9	98.9	1
Nova Scotia	99.3	52.4	46.9	99.9	99.1	0.8
Prince Edward Island	100	33.3	66.7	99.9	99.9	0
Newfoundland and Labrador	95.4	49.6	45.8	99.9	89.9	10
Yukon	0	0	0	99.9	86.8	13.1
Northwest Territories	0	0	0	99.9	84.4	15.5
Nunavut	0	0	0	99.9	99.6	0.3

Table 1.1: Percent of rural households in each province and territory where 50/10/unlimited FB service is available and LTE coverage is available [3].

rural homes and businesses can participate in the online ecosystem. In the future these limitations will also restrict the possibility for rural industries to take advantage of emerging technologies, such as the internet of things (IoT).

The Government and other advocacy groups recognize the challenges faced by rural users and have formulated policies to attempt to bridge the digital divide in these communities. Historically, these policies have laid the primary responsibility on network operators by mandating network investment in rural locations and specifying minimum service requirements. Often it has been assumed that business cases could motivate such investment, but, in recognition of the prohibitive costs, the Government of Canada has also provided large subsidies to operators. In spite of these subsidies, the cost to build robust networks at scale remains high, especially for wired FB services. Therefore, a significant portion of rural Canada remains poorly connected at home. Indeed, as recently as 2019, over 25% of rural households in Canada had no ability to access wired Internet connections at all, and were solely dependent on some form of fixed wireless technology (e.g., satellite, 802.11 point-to-point, 4G fixed wireless access) to get online [3].

Focusing now on wireless, it is interesting to note that mobile network operators (MNOs) have made significant investments in rural communities in Canada, and today, over 95% of rural households[2] nationally have 4G LTE coverage [3]. Table 1.1 shows the regional breakdown of urban vs. rural LTE availability.

[2]The CRTC measures rural LTE coverage with respect to the percentage of households that have LTE coverage.

Thus, in general, the mobile broadband divide between urban and rural communities is significantly smaller than the FB divide.

Historically, fixed and mobile broadband communications were provided by separate technologies, different providers, and evolved differently from one another. However, recently, the high level of cellular coverage has begun to lead to a convergence between mobile and FB services with fixed wireless access (FWA) being offered to provide FB using cellular infrastructure. This makes the infrastructure "multi-service", i.e. offering mobile and FB, which creates a host of new challenges that are the focus of this thesis.

In cellular FWA, rural homes or businesses are equipped with roof mounted, high gain antennas (Figure 1.2). An MNO can assist with the installation of the antenna to achieve line of sight (LOS) to the best base station (BS). Connected to each antenna is a modem with a SIM card (in this sense, each home or business is a user equipment (UE) associated with one cellular FWA subscription), which provides FB services to users within the premises.

FB services differ from the types of services typically offered in mobile networks. In particular, IPTV is often a major component of FB, and since screens used for video streaming are much larger at home, the data rate requirements are high. In addition, small businesses (and possibly homes) might host servers, putting more pressure on the uplink. Typically, a minimum bit rate (MBR) would need to be offered to each subscribing home on both the DL and the UL as is loosely the case with other wired FB technologies; however, MBR requirements have not historically been present in mobile services.

Despite its strength as a mobile service, 4G is limited in what it can offer as a household FB service. Indeed, the existing availability of bandwidth and relatively simple MIMO and beamforming capabilities of 4G could make it difficult to serve very many FB users concurrently and could limit their bit rates (relative to newer wireline technologies) especially at the cell edge. Thus, despite the fact that 4G service is nearly omni-present in rural communities, 4G FWA is incapable of solving the rural digital divide.

On the other hand, the recent emergence of 5G brings enhanced broadband capabilities. 5G has new mid-range and mmWave bands, and can allocate much larger bandwidths to users on new or existing bands (up to five times the bandwidth of LTE for low-to-mid range bands and twenty times the bandwidth for mmWave bands [5–7]). Moreover, 5G has multi-user massive MIMO (MU-MIMO) and more sophisticated beamforming techniques that enable channels to be used more efficiently than LTE. Therefore, given the already extensive cellular coverage in rural communities, the connectivity gap between rural and urban FB users could be narrowed significantly by deploying 5G at existing rural 4G sites and providing 5G-based FWA services. Beyond the radio access network (RAN), 5G also

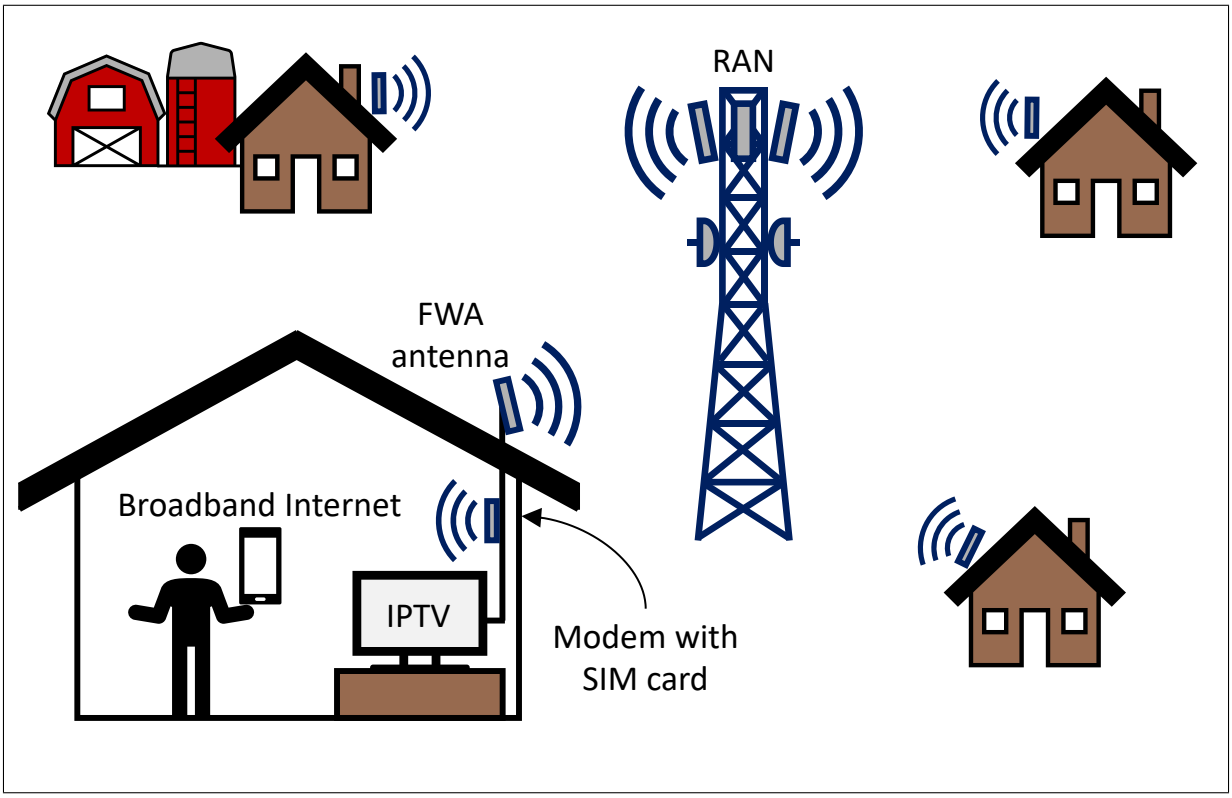

Figure 1.2: Rural Fixed Wireless Access

brings advancements to the backhaul, network edge, and core network that could make it a viable technology for providing robust connections to fixed, mobile, and IoT devices in rural areas.

Note that 5G FWA has already started being offered in urban areas using mmWave technology [8]. This has enabled users to combine their services and subscriptions in new ways, e.g., by bundling mobile plans together with home services. Hence, 5G FWA will not only improve the rural QoE, but is also likely to provide rural users with better contracts and service options.[3] Nonetheless, rural FWA has different challenges than urban FWA due to the relative scarcity of network resources and lower density of users, and will most likely use different bands (e.g., mid-bands) to cater to different requirements, including

[3]The reality is that 5G FWA will also improve the urban FB experience, and it is possible that the difference in data rates available to urban and rural households will persist. This is why we define the digital divide with respect to a certain minimum standard of acceptable service, i.e., the universal service objective.

greater coverage.

1.2 Contributions

In this thesis, we study how 5G FWA could solve the FB digital divide problem in rural communities.

In Chapter 2 we present 5G FWA in detail and outline many new advancements that 5G brings compared to earlier cellular technologies. We describe how these advancements could effectively enable cellular FWA in rural communities so as to narrow the urban-rural digital divide. In our review of these advancements, we focus on each section of the 5G network: the access, backhaul, network edge and core network. These advancements bring exciting opportunities for rural FWA users; however, MNOs providing this service to rural communities also face many new challenges. Hence, the second focus of the chapter is to discuss many of the open challenges that arise when considering how 5G MNOs can plan and operate their networks for FWA customers.

In Chapter 3 we study how MNOs can plan rural 5G MU-MIMO networks to provide MBR services to rural FWA homes jointly in the DL and UL. Specifically, we answer the following research questions: **RQ1:** Given a set of network resources, what is the user limit, i.e., the maximum number of homes that can simultaneously receive a target DL MBR and target UL MBR (or better)? **RQ2:** How should a network be configured to obtain such user limits? How should resources be shared between the DL and UL and how should users be selected? To answer these questions, we propose a static user grouping strategy that organizes homes into fixed groups and allocates an equal share of resources to each group. Under the static grouping strategy, we develop a simple process to determine the user limit by decoupling the DL and UL problems and determining the minimum number of resources required to give a group of users the MBR. We first study how DL and UL group sizes impact performance and show that smaller group sizes enable more streams to be used and a larger total number of users to be given the MBRs. Using the simplified planning process we developed, we then show how the user limit at different cell radii is impacted by the following: the system bandwidth, the number of antennas at the BS and homes, the BS transmit power, and the DL and UL MBRs. Finally, we show how these results can also provide insight into how the network should be operated when the number of active homes is less than the user limit.

1.3 Outline

The remainder of the thesis is structured as follows. In Chapter 2 we provide an overview of the new enhancements in 5G that are most likely to help narrow the rural digital divide; then we discuss a number of open research challenges that remain to be addressed in FWA-oriented rural 5G networks. Chapter 3 studies a problem introduced in the previous chapter of planning a 5G FWA network to provide MBRs jointly in the downlink and uplink. The chapter also provides some initial insight into how a 5G network could be operated to provide MBR services to FWA homes. In Chapter 4 we conclude the thesis and discuss some future research directions.

Chapter 2

Can 5G Fix the Rural Connectivity Gap?

2.1 Introduction

As mentioned in the previous chapter, mobile and FB have historically been provided through different technologies, with mobile services coming through cellular technologies and FB coming from wired technologies. However, the convergence between mobile and FB created by FWA results in a cost-effective alternative to wired FB in rural communities. To date, initial 4G-based FWA deployments have not been able to sufficiently narrow the rural-urban FB digital divide. In this chapter, we argue that the emergence of 5G can significantly narrow that gap through 5G FWA, and 5G could further enable the adoption of IoT in rural industries. Indeed, 5G brings advancements to the access, backhaul and network edge that will make it a viable technology for fixed, mobile, and IoT applications in the rural context; so much so that it is anticipated that Mobile Network Operators (MNOs) could dominate the rural Internet market in the future. One objective of this chapter is to present 5G FWA in detail and outline the 5G advancements that will benefit FB users in rural areas (the other services are only mentioned briefly), focusing on each of the access, backhaul and network edge.

So far, most work on 5G FWA has focused on the use of mmWave spectrum, largely in urban areas [8–10]. However, rural FWA has different challenges and opportunities than urban FWA. In mobile contexts, the challenge was typically to provide capacity in urban environments and coverage in rural ones. However, MNOs offering FWA to rural areas will face both coverage and capacity challenges since they need to be able to provide MBRs to

homes on both the DL and the UL. On one hand, rural FWA is expected to be LOS, where the MNO installs a roof-mounted array of antennas at each home and points it directly at the BS, and rural sites have much lower inter-cell interference. Rural FWA will also serve a lower density of spread out homes, which is an ideal environment for MU-MIMO [11,12]. On the other hand, rural channels have fewer multipath components that can be exploited, and it remains unclear how useful mmWave will be for rural FWA given its propagation characteristics. Some claim that rural 5G FWA could use mmWave [8,13,14], but there are limitations to these works: [8] states the assumption without verification, [13] only verifies it in a suburban context, and [14] finds that mmWave cannot practically provide FWA service beyond a 1500 m cell radius, which might be too limited a distance in practice. We focus on the use of mid-band FWA, which has less bandwidth than mmWave, but can provide larger coverage distances. Others suggest that mid-band spectrum, such as 3.5 GHz, will be widely adopted for rural FWA [15,16]. What is clear is that rural FWA creates exciting opportunities and new challenges for MNOs. The second goal of this chapter is to highlight the open challenges and questions MNOs would face in planning and operating a rural converged 5G network.

We structure the remainder of this chapter as follows: First we describe the relevance of 5G to the rural digital divide problem in Section 2.2. Focusing on each section of the network, we describe the improvements brought by 5G that are most likely to help address rural connectivity challenges, specifically in the context of FWA. Next, in Section 2.3 we examine a number of open challenges to bridging the rural digital divide through 5G FWA, focusing on network planning and operation of multi-user massive MIMO FWA networks, challenges in the backhaul, and coexistence with other legacy technologies and MNOs. The chapter is concluded in Section 2.4.

2.2 How 5G Can Help the Rural Digital Divide

5G builds upon decades of past work on earlier generations of cellular communications and brings vast improvements to data rates, latency, mobility management and energy efficiency. At the same time, 5G revolutionizes cellular technology in that it no longer aims to be a service catered to personal mobile communications only. Indeed, 5G is intended to offer diverse types of services with different requirements. The service types are broadly classified as enhanced mobile broadband (eMBB), massive machine-type communications (mMTC), and ultra-reliable low-latency communications (URLLC) [17].

eMBB is the natural evolution of mobile broadband from the 4G era, providing enhanced data rates to a larger number of users with possibly higher mobility. eMBB en-

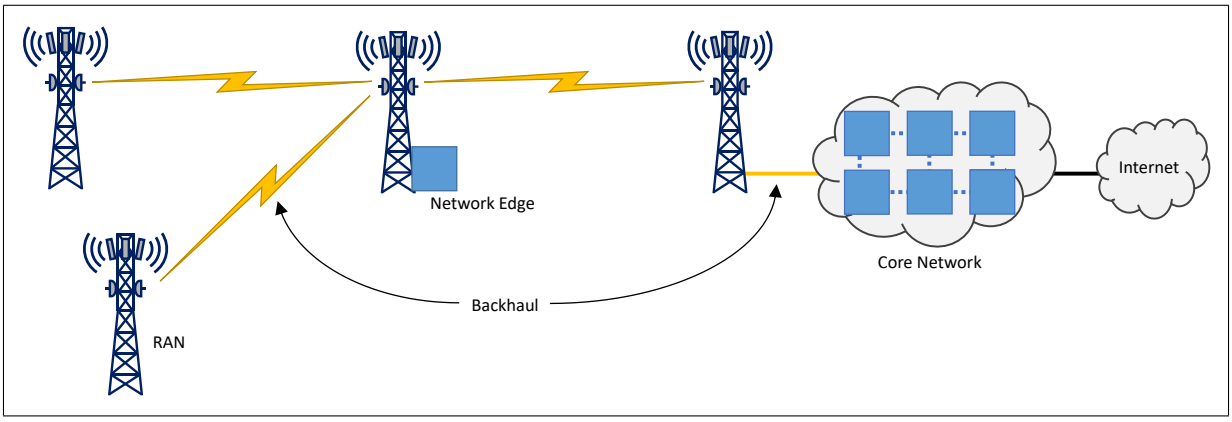

Figure 2.1: 5G network architecture

compasses more than smartphone technology and includes the FWA services we focus on in this thesis. Before 5G, cellular has not been a viable technology for providing consistent high-rate services, such as IPTV at scale. However, due to the enhanced data rates that will be made possible with 5G eMBB, we can envision a large-scale convergence of cellular and fixed access for the first time.

mMTC enables the connectivity of massive numbers of low-cost, highly energy-efficient IoT devices, such as industrial sensors. URLLC applies to contexts with unprecedented latency and reliability targets, such as vehicle communications, remote medical applications, and some industrial applications. In the rural context, mMTC will enable the adoption of IoT in rural industries while URLLC may drastically change how medical care can be provided to rural communities that lack on-site medical specialists.

To meet the stringent requirements for each service type, 5G brings improvements to every area of the network architecture illustrated in Figure 2.1, including the *radio access network (RAN)*, the *5G core network (5GC)*, which provides end user functionality for mobility, billing, and other services and which is a gateway to external networks, the *backhaul* that interconnects the RAN and 5GC, and the so-called *network edge*, which enables data, applications and other specialized network functions closer to end users, somewhere between the 5GC and RAN, in order to improve QoE.

The shift toward FB services through FWA will require 5G MNOs to provide a well-managed, end-to-end service. Hence, the advancements in each area of the network will be critical to making 5G FWA a success in rural regions. We now describe how these improvements will help solve the rural digital divide problem.

2.2.1 Access

Advances in (multi-user) MIMO and beamforming technologies, a new radio air interface 5G NR [18] and the availability of new parts of the wireless spectrum enable the offering of significantly higher data rates to a significantly higher number of users per cell.

One of the key advancements in 5G is multi-user massive MIMO (MU-MIMO), which has the potential to provide a tenfold increase in system capacity over single-user MIMO used in 4G [19]. In massive MU-MIMO, BSs equipped with large numbers of antennas (10s to 100s) can transmit to or receive from multiple users in the same resource block [19]. This multi-user transmission is enabled by the combined gains from spatial multiplexing, improved signal energy from antenna beamforming, and reduced interference due to precoding at the transmitters and combining at the receivers. Together, these benefits give rise to a much higher Signal to Interference plus Noise Ratio (SINR) and hence better rates, particularly for cell edge users. 5G MU-MIMO is therefore essential for the rural FB context since high rates and good coverage are both needed. MU-MIMO is especially well-suited for the rural FWA scenario given that homes are non-mobile and likely to be well-separated from one another, which is advantageous for beamforming [11, 12]. The benefits of MU-MIMO come at the cost of increased complexity, however, which influences how effective the technology will be in the FWA context.

The 5G New Radio (NR) interface is designed to be flexible and efficient to meet varying network environments and diverse requirements of eMBB, URLLC, and mMTC users. To this end, 5G NR enables operators to configure different channel frame structures depending on the need [17,18]. The NR radio frame supports various subcarrier spacings, giving rise to different OFDM symbol durations. This enables shorter time-slot durations, which will enable shorter transmission time intervals and, hence, lower latency transmissions. This flexibility is also necessary for 5G to support mid-bands and new mmWave bands, which have very different Doppler characteristics.

Historically, frequency division duplex (FDD) bands were dominant in LTE, which assigned equal bandwidth to the DL and UL. With 5G, however, time division duplex (TDD) is generally expected to be the main duplex technology as the majority of the new bands supported by 5G will be TDD bands (both mmWave and mid-bands, such as 2.4 GHz and 3.5 GHz). In general, TDD provides more flexibility than FDD since the share of time resources between the DL and UL need not be equal. This makes TDD better-suited for asymmetric, DL-heavy services, such as FB.

NR TDD has multiple strengths over FDD (NR or LTE) and LTE TDD. NR TDD supports user bandwidths up to 100 MHz for sub-6 GHz bands and up to 400 MHz for

mmWave bands [6, 7]. For comparison, most NR FDD bands support a maximum bandwidth of 20 MHz (although some allow up to 50 MHz) [6], while LTE (TDD or FDD) only supported a bandwidth up to 20 MHz. NR TDD also has much greater flexibility than LTE TDD. In LTE the TDD configuration (i.e. the ratio of time-slots given to the DL vs. the UL) was static (or at least semi-static) and needed to be coordinated between neighbouring cells to prevent interference. However, in 5G, TDD configurations can change from slot-to-slot [20] and there is no hard requirement to use the same configurations between neighbouring cells (though there is ongoing work on how effectively the resulting interference would be managed [21, 22]). This flexibility is designed to make it possible for operators to serve diverse and sometimes conflicting user requirements, e.g. DL-heavy FB vs. UL-heavy IoT applications. In a FB scenario it also means that an operator could dynamically adjust the time configuration to maximize the quality of experience (QoE) given to each home.

5G has access to an abundance of new spectrum [17]. Most notable are the mmWave bands; however, given its propagation characteristics, it is unclear how well mmWave will benefit rural users. Nonetheless, the new sub-6 GHz bands (i.e., mid-bands) that have been made available seem well-suited for the rural context. Beginning with Release 16 of 5G, access to unlicensed spectrum is also made possible [23]. Although proper interference coordination is required for unlicensed access, it is anticipated that this coordination will be easier to manage in sparse regions with fewer interference sources; hence, unlicensed spectrum may be highly beneficial in rural regions.

Aside from newly available spectrum, MNOs might also have access to the portion of their regular bands that they are not using in rural regions. Typically, this has been because the extra capacity was not needed in these regions. In this case, the bands can be readily deployed to add capacity to rural sites for FWA. In other cases, some higher-frequency, sub-6 GHz bands have been unused in rural regions because of their poor characteristics for mobile communications. However, these bands might be useful for FWA since FWA homes will have roof-mounted, high gain and high transmit power antennas that can handle these bands more effectively than mobile devices.

2.2.2 Backhaul

The backhaul has a direct impact on the performance of the RAN and therefore on QoE given to end users. In fact, unless the capacity of the backhaul is scaled up to accommodate the RAN, efforts spent increasing capacity in the RAN with MU-MIMO, 5G NR, and new bands will be wasted. In rural areas, backhaul has usually been provided using microwave

point-to-point (MWP2P) technology [24], which is a cost-effective solution for providing low-to-mid data-rates over long distance hops. To increase the capacity of the backhaul, similar approaches (e.g., MIMO, new bands) as those presented above for the RAN can be used.

Starting with Release 16, it is possible to establish backhaul connections between neighbouring BSs using the same antennas, bands, and radio protocols that are used to provide user access in the RAN. In other words, sites can be self-backhauled without requiring MWP2P or fibre backhaul technology. This new functionality is called integrated access and backhaul (IAB) [23, 25] and it might be very useful in rural areas. IAB is designed to use TDD spectrum in both sub-6 GHz and mmWave bands. Given the asymmetric nature of broadband traffic, the ability to have a TDD-based backhaul could be advantageous for FWA in comparison to MWP2P, which utilizes FDD channels.

IAB has two modes: in-band and out-of-band. In-band IAB uses bands which are shared with user access. Hence, it treats a connected BS like any other UE on the downlink, meaning the BS must be scheduled alongside users. In-band IAB nodes cannot transmit to users while receiving data from another IAB node (i.e., operation is half-duplex). Out-of-band IAB uses dedicated bands for backhauling. In the rural context, MNOs might find out-of-band IAB to be a way to put currently unused spectrum to good use. The two IAB modes are depicted in Figure 2.2.

2.2.3 Network Edge and Core Network

To improve connection robustness and latency, and hence perceived QoE, for both URLLC applications and eMBB users, MNOs need to be able to move control plane functionality as well as user content (via caching) closer to the network edge. This would also reduce the traffic on the backhaul, an added benefit.

This requirement to do things locally is not new to 5G, nor is it unique to the rural context; however, the virtualization (through network function virtualization (NFV)) of the 5GC makes it easier to distribute functionality closer to the network edge than before and makes it possible to do so at *lower cost* and in a *scalable manner* [26]. This will be essential for providing the functionality necessary to meet URLLC and mMTC service requirements, and will enable the adoption of IoT in rural industries. Furthermore, it will be key to providing seamless mobility and more responsive connections to rural eMBB users.

Similarly, multi-access edge computing (MEC) will enable operators to cache user content closer to rural sites and move application servers to the network edge, improving

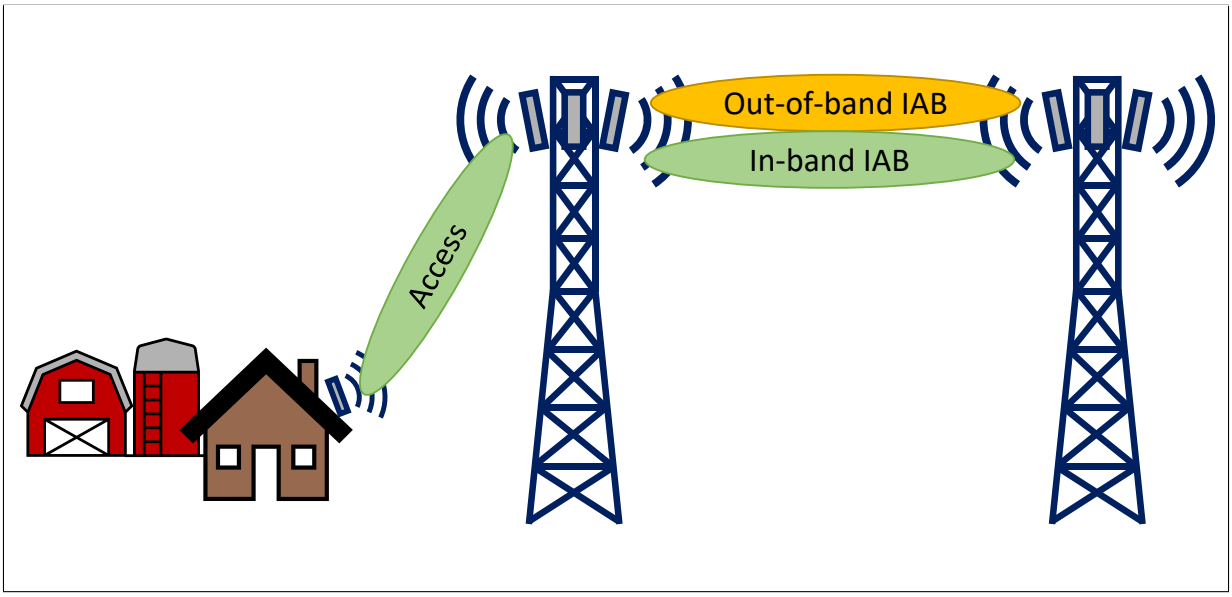

Figure 2.2: Integrated access and backhaul (IAB) makes use of NR access technology to provide backhaul connections between neighbouring BSs. In-band IAB shares its spectrum with the RAN. Out-of-band IAB uses dedicated spectrum.

responsiveness and download times for FWA and mobile users as well as reducing traffic and signalling loads on the backhaul [27]. This will require cooperation on the part of content providers and application developers, who might be motivated to help in this way out of recognition of the benefit to end users. Nevertheless, some parties might be unwilling to help out of good will, in which case the involvement of regulators might be necessary [28].

2.3 Open Challenges to Fixing the Rural Digital Divide Using 5G

To enable 5G FWA in rural areas, a number of open challenges remain to be solved, which we now discuss.

2.3.1 Network Planning and Operation for 5G FWA

The focus on providing home-oriented services, such as broadband Internet and IPTV, for FWA users will require MNOs to plan and operate their networks differently than in the past when services were oriented around mobile users.

It is expected that service level agreements (SLAs) between MNOs and their subscribers will establish different commitments for different services; for example, an MBR for FB Internet service on both the downlink and the uplink (although different values), or a guaranteed IPTV service. The first challenge is thus a planning (or dimensioning) problem. As always, there exists different flavors of the planning problem but we expect that, initially at least, the placement problem can be avoided by using the existing 4G infrastructure. Selecting the right band(s) is critical to 5G FWA, and the first problem is determining how many homes can be offered FB for those bands. Specifically, given a fixed amount of access and backhaul resources (e.g., band(s), per band bandwidth, transmit power, characteristics of the massive MIMO antennas at the RAN and homes), an MNO needs to determine the number of homes that can be given the MBRs. Note that this problem is difficult at many levels and in particular because it involves MU-MIMO (hence the need for precoding and combining), and couples the uplink and downlink and the RAN and backhaul. As was mentioned earlier, 5G provides an abundance of capacity improvements in the RAN due to enhancements from massive MIMO and new spectrum; however, unless the backhaul is also sufficiently dimensioned, the improvements that the RAN can bring to the end-user QoE will not be fully realized (this will be discussed in Section 2.3.3). A similar problem exists for legacy wired broadband technologies; however, the challenge in the cellular context is that data rates change based on the environment, the position of users, and the network load, which is why MNOs have historically only provided best effort services. For this reason, an MNO might determine that the MBRs in an SLA should differ depending on the home location.

MNOs must understand the benefits of adding more antennas at the RAN or at the homes and the importance of transmit power. The large coverage requirement in rural areas could cause a power imbalance between the uplink and downlink. This also must be studied since it could result in an imbalance with respect to the number of homes that can be given their MBR in the uplink vs. the downlink. In earlier generations, the placement of BSs was done for mobile services to strike the right trade-off between data rates and coverage. However, the right trade-off for 5G FWA might well be very different and hence, if 5G FWA becomes successful in rural areas, it might be necessary to address the question of where and how to add BSs for accepting more FB subscribers.

Another open issue is related to the sharing of bands between mobile services and

FB services. Is there an advantage to segregating the services (possibly through network slicing) or is it better to keep services together for better statistical multiplexing? This is very much related to how the network will be operated.

If a network is properly dimensioned, an operator should *in theory* be able to fulfill SLAs for every home, irrespective of how many homes are active. On one hand, when few homes are active, it might be easy to offer the homes their MBR, in which case the next objective is to offer extra rates with the surplus resources in a fair fashion. On the other hand, to give every home the MBR when many homes are active would require a well-designed scheduler. Designing a scheduler for MU-MIMO that protects the different services and is backhaul and SLA-aware is challenging, and a good compromise in terms of performance and complexity needs to be found.

Finally, note that similar questions exist for mMTC and URLLC.

2.3.2 Compatibility with Legacy Technologies

While we view 5G as a long-term solution for the rural digital divide, it will be some time before MNOs can fully deploy 5G to rural locations so that communities can depend on it exclusively. Nevertheless, most rural communities already have infrastructure in place from earlier legacy broadband technologies, such as DSL or cable. Thus, there will exist a period—at least temporarily, and possibly longer-term—where 5G coexists with older networking technologies in rural communities. A key challenge then is how to deal with this heterogeneity in the network in a way that ensures the best possible QoE for users. These kinds of problems are rarely addressed by the research community while they often plague the engineers in charge of deploying such systems.

This potentially yields a situation where homes are connected to two networks, one cellular and one wired. This dual access introduces a number of complexities due to the use of different technologies (in both the access and the backhaul) and due to the heterogeneous link characteristics (e.g., bandwidth, latency, packet loss). This dual access can be handled by a box installed at the home that selects one technology or both. Note that the entity in control of the box could be the 5G MNO, the legacy operator or a third party. This would impact what is possible. The technology selection might be defined by static policies, such as the type of application or time of day; however, adaptive steering based on the quality of service (QoS) of each link would be able to provide better QoE to users, though it would be more difficult to implement. Because link QoS and user flows are dynamic, mechanisms are also required to hand users over from one technology to another, possibly mid-connection, without disrupting QoE.

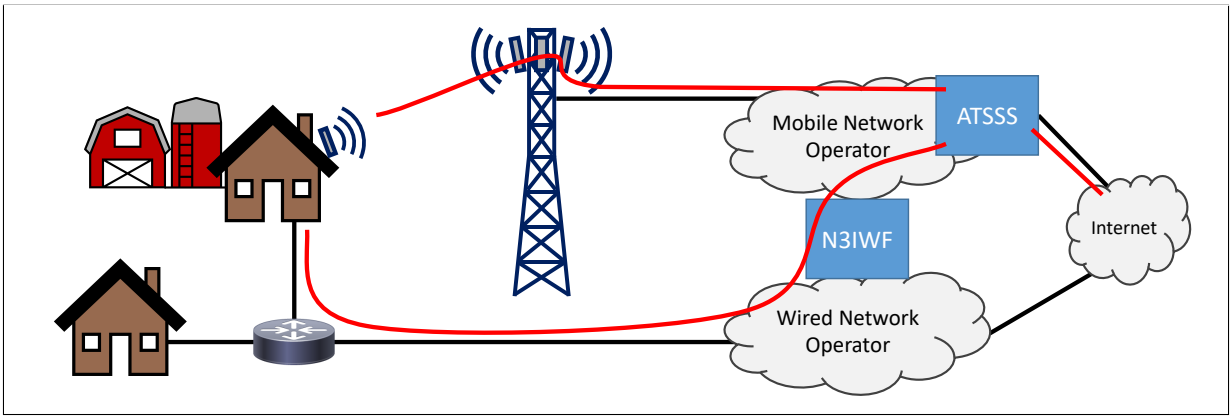

Figure 2.3: 5G Access Traffic Steering, Switching, and Splitting (ATSSS) functions could enable dual connectivity between 5G and legacy technologies at rural homes.

To support simultaneous use of 5G FWA with a legacy technology, the box will need to support multipath protocols, such as multipath TCP (MP-TCP). However, MP-TCP is less effective when connection paths are more heterogeneous, which can cause head-of-line blocking issues [29]. To avoid this problem, multipath QUIC [30] could be used, but it presents its own challenge to operators: specifically, it limits how effectively network operators can utilize proxies or caches in the network [28, 31]. In recognition of this limitation, extensions to QUIC have recently been proposed as workarounds to this issue [31].

Clearly, implementing an MBR in a heterogeneous context is challenging—if at all possible—and would depend, among other things, on which entity is in control of the box.

In Release 16, 3GPP has introduced functionality to support dual connectivity with non-3GPP technologies through a new set of functions called Access Traffic Steering, Switching, and Splitting (ATSSS) [32]. Here, steering, switching, and splitting refer to the network selection, handover, and aggregation described above, respectively, where the entity in charge is the 5G MNO. ATSSS functionality is located within the 5GC and at the UE (i.e., the FWA modem) as shown in Figure 2.3, and operates alongside another new function called the Non-3GPP Interworking Function (N3IWF), which acts as the point of convergence between the non-3GPP network and the 5GC.

An important feature of 3GPP ATSSS is that all user traffic is tunneled through the MNO's 5GC and the ATSSS policies are defined by the MNO. Thus, ATSSS puts control on the 5G side, making it much easier for MNOs to monitor instantaneous rates given to dual-connected users and implement policies to ensure SLAs are satisfied.

For operators that have cellular and wireline networks, ATSSS functionality could prove

very useful for effectively using their legacy network alongside 5G. However, for the case where standalone legacy operators provide dual-access with 5G MNOs, the legacy operators are required to forfeit control over to the MNOs. One alternative might be to have a neutral third party host the core network functions that are necessary for convergence and coordinate policies between the two operators. Virtualization would make such an arrangement with a neutral host scalable.

In the end, the 3GPP/non-3GPP dual-access problem is difficult to generalize and might be best solved with coordination among the applicable industry consortiums. ATSSS is just one possible solution, but it is still a nascent technology, and 3GPP is working alongside the Broadband Forum and CableLabs to standardize the functionality for DSL and cable, respectively.

2.3.3 Backhaul Challenges

The MBRs expected from the RAN can only be delivered if the backhaul is also dimensioned appropriately. Until now, the backhaul has been dimensioned for mobile users, which have no MBR expectation. However, FWA services will require MNOs to make significant upgrades to their backhaul. As mentioned earlier, rural backhaul links are primarily based on MWP2P technology, which is licensed per channel and per hop. Due to the low amount of long-range MWP2P spectrum that remains unused, it could become increasingly difficult for MNOs to secure sufficient channel licenses for their rural backhaul links in order to meet the QoE for FWA.

Despite the introduction of IAB in 3GPP Release 16, it is unlikely to become a primary backhaul technology for rural BSs. Rural backhaul needs to be long-range while IAB is mainly envisioned to use wide-bandwidth mmWave bands to create a short-range backhaul alternative to fibre or MWP2P [25]. Even though IAB also supports use of sub-6 GHz bands, fewer of these bands are available and they are lower bandwidth, which limits their viability as an independent backhaul solution. Nonetheless, one possibility we see is IAB being used to provide additional backhaul capacity on top of existing MWP2P backhaul in specific areas with low density of subscribing homes. This is one way in which MNOs could utilize currently unused access spectrum. In considering this, MNOs must understand under which conditions (in-band or out-of-band) IAB is a good alternative to adding MWP2P backhaul capacity.

The primary challenge with a dual IAB-MWP2P backhaul approach is that it falls outside the scope of current specifications: so far IAB has been specified as a standalone

backhaul technology with no specification for its coexistence with other backhaul technologies. This is likely due to the wide differences in how backhaul functionality is deployed in each technology: IAB employs many of the same protocols and scheduling mechanisms that are used for access in the RAN, while MWP2P has its own set of protocols. Nonetheless, as there has been steps towards convergence between 3GPP and non-3GPP access, it might also be worth studying the coexistence of heterogeneous backhaul technologies.

Assuming this coexistence, there would be similar challenges as in the access in terms of backhaul selection, aggregation, and handover during traffic flows.

2.3.4 Infrastructure Sharing

Frequently, MNOs serving the same geographic regions will share infrastructure to reduce costs. Depending on which parts of the network are shared, these schemes may be classified as:

1. Multi-operator RAN (MORAN), where each operator uses its own access band(s) but share BSs and backhaul links.
2. Multi-operator core network (MOCN), where the RAN (including the bands) and backhaul are fully shared.
3. Gateway core network (GWCN), which extends MOCN by also sharing some core network functionality, for example, mobility management functions.

Despite their added architectural complexity, MORAN and MOCN arrangements found wide use in the past due to their effective cost reductions. Nonetheless, in the context of 5G networks that will promise MBRs to FWA subscribers, it could be very challenging for competing operators to provide service guarantees over these types of shared networks. For example, MNOs may bring different resources (e.g., amounts or types of spectrum for the access and backhaul, computational resources, etc.), so a key challenge is to share these resources in a way that is fair to operators (and hence, users) while also preventing free-riders. Considering this, advancements in 5G network slicing, enabled by virtualization and edge computing, are expected to introduce new opportunities to sharing [33]. With regards to MEC, it is more efficient for MNOs to utilize shared caches and application servers in rural communities; however, this leads to new challenges in terms of content storage policies for copyrighted material, data privacy, or any other special agreements between MNOs and content or application providers.

One way to address the new challenges in virtualized multi-operator scenarios might be to adopt frameworks in which a neutral third party acts as a broker to ensure fairness between all of the involved parties.

2.3.5 Remote Digital Divide

In spite of the promising benefits of 5G FWA, it could be insufficient for solving the digital divide in Canada's most remote communities. Like elsewhere, local FB access in these communities is provided to homes through wired or fixed wireless technologies; however, the geographic isolation of these communities makes it so that satellite is the only practical way of backhauling connections. Hence, each community has a shared satellite gateway to backhaul connections into the community. Figure 2.4 shows the remote communities in Canada that are dependent on this type of architecture.

For these communities, the backhaul forms the bottleneck in connections due to the high latency and narrow bandwidth of the satellite link. Hence, latency is also a significant issue in addition to rates. Operators in remote communities are therefore particularly limited in their ability to improve the experience of users, regardless of the benefit 5G FWA could bring to local access within the communities.

To minimize the impact to end users, remote community operators need to carefully manage signalling and traffic over the satellite link. In the past, this was accomplished through caching and proxy-based solutions. Given the richness and complexity of modern web content and applications, these solutions are more essential than ever and MEC will be an important part of this; however, remote operators face a losing-battle, especially as content providers and application developers are increasingly taking control of connections through encryption and more sophisticated web protocols. Hence, the experience of users in remote, satellite-dependent communities risks getting worse unless content providers and application developers also become closely involved to fix the issue. We describe our vision for how the remote digital divide can be addressed in an earlier paper [28]. Additionally, new enhancements under discussion for 5G Release 17 are intended to target deep rural environments served by satellite or other non-terrestrial links [23].

2.4 Conclusion

5G FWA is a paradigm shift that will enable more to be done using cellular technology than ever before. In this chapter, we have argued how new advancements 5G brings to

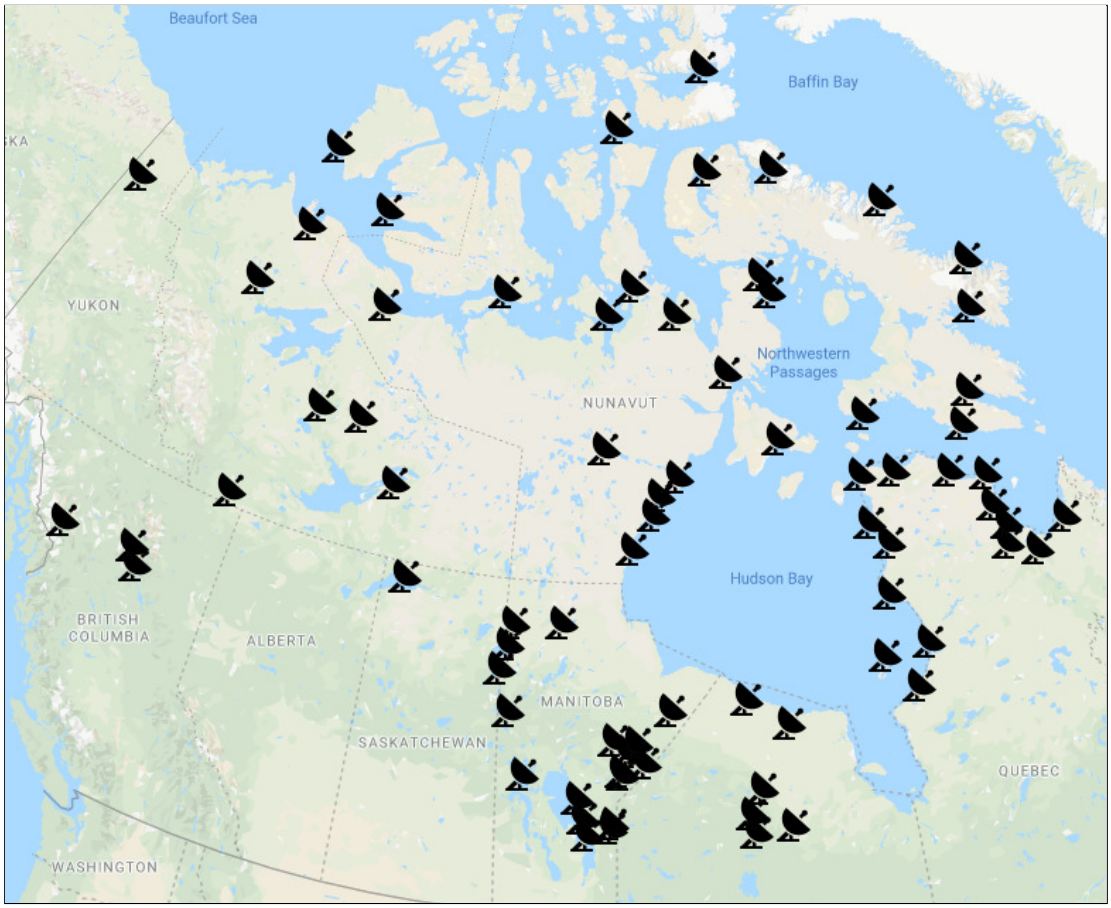

Figure 2.4: Communities in Canada where satellite is the only medium over which users can connect to the Internet. Adapted from [34]. Map data ©2020 Google, INEGI.

the network access, backhaul, edge and core each present new opportunities for narrowing the digital divide in rural communities in the context of FWA users. However, out of these opportunities also arise new challenges related to network planning and operation, and coexistence alongside legacy technologies and other operators. Can 5G fix the rural connectivity gap? We believe that it can in time and that FWA could be a significant step towards bridging that divide. However, there is still plenty of work to be done by the research community before the gap can be completely filled.

Chapter 3

Planning 5G Networks for Rural Fixed Wireless Access

3.1 Introduction

In this chapter we seek to answer some of the questions raised in the previous chapter related to how operators can plan rural 5G MU-MIMO networks so that rural FWA homes can be offered MBR services jointly in the DL and UL. In particular, we seek to answer the following two questions: 1) Given a set of network resources, what is the maximum number of homes that can be served simultaneously in a cell such that they receive a DL MBR and UL MBR (or better)? 2) How should a network be configured to obtain such user limits? In particular, how should resources be shared between the DL and UL and how should users be selected?

We consider a single cell 5G MU-MIMO system using a 3.5 GHz TDD band, in which homes have multiple antennas supporting multi-stream transmission and reception. In a rural scenario, inter-cell interference can be neglected so we focus on a single cell scenario. Our first objective is to understand the user[1] limit (i.e., the maximum number of rural FWA homes that can be offered the DL and UL MBRs simultaneously) given a certain cell radius, a certain bandwidth, DL and UL MBRs, a number of antennas at the BS M_{BS} and at each home M_{H}, and a certain power at the BS and homes. Because the system is TDD, DL and UL resources are shared in time, where the UL gets T_u out of T slots

[1] A modem installed at the home contains the SIM card associated with a FWA subscription; hence the home can be thought of as a user equipment.

in a frame, and the DL gets the remaining $T_d = T - T_u$ slots. For this reason, the DL and UL problems cannot be studied independently: this is a joint problem in which it is necessary to determine how many resources are used for the DL vs. the UL. Hence, a related objective is to determine what value of T_u is necessary to attain the user limit.

The fulfillment of these objectives depends on different radio resource management (RRM) procedures at the Physical Resource Block (PRB) level, such as user selection, i.e., which homes (and streams) are scheduled, the precoding and combining that apply beamforming to each stream at the transmitters and receivers for the selected homes, the power distribution (PD) applied to each stream, and the modulation and coding scheme (MCS) selection per stream, which determines the data rate based on the channel conditions. To help fulfill our objectives a joint optimization problem can be formulated for a given realization $\omega(U)$, which is characterized by a randomly distributed set of U FWA homes and their channel matrices, to check if there exists a T_u, user selection, precoding/combining, PD, and MCS selection for which $\omega(U)$ is feasible (i.e., for which the MBRs can be offered to all U homes on both the DL and UL). However, the resulting problem is very large and complex, and to obtain meaningful limits and configurations it would need to be solved for different values of U and for many realizations for a given U, which is too heavy.

To simplify the problem we adopt block diagonalization (BD) precoding and combining in both the UL and DL. BD limits the number of homes that can be transmitted to on the DL or that can transmit on the UL to $N = \left\lfloor \frac{M_{\text{BS}}}{M_{\text{H}}} \right\rfloor$ [35], which could be small in an FWA system where homes have multiple antennas. However, MNOs need to support a large number of homes, and thus the user limit should not be limited by N. Hence, we *cannot* assume that all homes can be transmitted to or from in each PRB and we must adopt some strategy to properly select users. Dynamic, per-PRB user selection strategies could accomplish this, but these are complex. Instead, we adopt a static user grouping strategy, which organizes homes into fixed groups of size $S_d \leq N$ in the DL and $S_u \leq N$ in the UL (S_d needs not equal S_u) and allocates an equal share of PRBs to each group. The static grouping strategy enables us to compute a user limit in a simple and robust manner making planning manageable. It is possible that in an operational phase a more flexible strategy would be more efficient.

Contribution 1: In the context of grouping, we first need to understand if we should always select N homes per PRB and how many streams should be selected per home. Our first contribution is to show that selecting N (or close to N) homes per PRB is generally not optimal. In fact, a greater number of homes can be given the DL and UL MBRs if we select fewer homes with more streams than more homes with fewer streams.

Contribution 2: By adopting the static grouping strategy, we develop a simple process

to determine the user limit for a given system setting. First, we (separately) determine the minimum number of subchannels needed to provide the DL and UL MBRs for different group sizes for a given T_u. Then, knowing the total number of subchannels available in the system, we use this information to determine how many groups can be given the MBRs on the UL and on the DL, and, consequently, how many homes can be given both MBRs for a given T_u. A search on T_u for different S_d and S_u then determines the correct configuration of T_u, S_d, S_u required to maximize the number of homes in the system. The elegance of this approach is that it enables MNOs to quickly dimension their network for a MU-MIMO FWA system with DL and UL minimum bit-rate requirements. Using this process, we show how the user limit at different cell radii is impacted by the following: the system bandwidth, the number of antennas at the BS and at the homes, the BS transmit power and the DL and UL MBRs. Note that it is possible that the user limit could be even larger if a more flexible user grouping was used, but the computation would become much more complex as explained later.

Contribution 3: Although our main focus is network planning, the results obtained can also indicate to MNOs which configuration of T_u, S_d, S_u are optimal when the number of active homes is less than the user limit. In other words, these results can provide insight into how the network could be operated. Specifically, we show that by adjusting the group sizes and slot configuration T_u based on the number of active homes, the DL and UL rates given to homes can be improved with respect to operating statically with the configuration that is necessary to obtain the user limit.

We structure the remainder of this chapter as follows. In Section 3.2 we review the related work. We describe the system model in Section 3.3. The problem formulation and the process to determine the user limits are presented in Section 3.4. In Section 3.5 we provide the numerical results, which answer the network planning questions and provide some preliminary insights to some network operation questions. We conclude the chapter in Section 3.6.

Notation: $\mathbb{R}$ and $\mathbb{C}$ denote the set of real and complex numbers, respectively. $\mathbb{R}_+$ denotes the set of non-negative real numbers. Vectors and matrices are shown by bold lower-case and bold upper-case letters, respectively.

3.2 Related Work

The authors of [36] and [37] provide an overview of network dimensioning and planning in 4G while looking ahead to 5G. They also summarize a number of classical references

on these topics. However, most of the earlier literature focused on the mobile context rather than providing a robust FB service at homes. More recently, [13] considered the BS placement problem to guarantee 5G FWA homes a minimum coverage level and DL data rate using mmWave cells. [38] also modeled the 5G BS placement problem to guarantee a minimum DL service level while simultaneously minimizing BS electromagnetic field power. In our problem, we assume that MNOs will reuse the existing 4G towers for 5G FWA, hence our focus is on quantifying the number of FWA homes that can be provided a MBR in both the DL and UL. Another recent paper used crowdsourced data to dimension existing BSs and determine the appropriate per-site NR configurations required to support new 5G services [39]; however, their dimensioning process was based on peak DL data rate requirements.

Although none of these recent works considered the UL in their problems, a couple past papers on 4G planning and dimensioning considered DL and UL service requirements jointly. [40] examined how 4G BSs could be planned to provide DL and UL MBRs while supporting ON-OFF switching to save energy. In their study, user limits were assumed to be known a priori, however. Furthermore, the system was FDD with fixed DL/UL bandwidths, and thus, did not consider the resource allocation problem. [41] studied the dimensioning and planning problems for 4G networks with DL and UL MBRs; however, the user limits computed in the dimensioning stage only took the DL MBRs into account and modeled the spectral efficiency as constant throughout the cell. Furthermore, neither of [40, 41] considered the effect of MU-MIMO.

The literature on resource allocation and precoding techniques for massive MU-MIMO is very rich and [42] presents a comprehensive survey on these topics. Recent work on MU massive MIMO beamforming for FWA applications was performed in [10, 43]; however, these papers considered mmWave bands only and a relatively small number of users. In the problem we study we adopt block diagonalization (BD) [35, 44–46] precoding and combining in the DL and UL, which generalizes zero-forcing (ZF) precoding to the case where the receivers have multiple antennas. The strength of BD is that it eliminates inter-stream interference at each UE, in addition to suppressing inter-user interference like ZF. BD is also simple to compute for an offline problem as in the network dimensioning problem that we study.

In the past, the problem of providing MBRs in MU-MIMO systems under BD or ZF precoding/combining has mostly been studied separately for the DL [47, 48] or the UL [49, 50]. The authors of [51] formulated the problem for both the DL and the UL of a MU-MIMO system but considered the two directions in isolation, thus ignoring the issue of providing MBRs to the DL and UL simultaneously.

A notable limitation of BD (and ZF) is that the number of users that can be selected together on a single Physical Resource Block (PRB) is restricted to $N = \left\lceil \frac{M_{\text{BS}}}{M_{\text{UE}}} \right\rceil$, where M_{BS} is the total antennas at the BS and M_{UE} is the total antennas at each UE [35]. To avoid this limitation, many papers modeling MU-MIMO systems simply assume that the total number of users is no more than N, and hence, all users can be selected simultaneously [10, 43, 47, 49, 50] (also, [42] and references therein). In FWA, homes have multiple antennas and, hence, the value of N might be small in practice. Therefore, to support a larger number of homes, user selection techniques must be implemented, which we study. Earlier work on MU-MIMO systems where the total number of antennas at the BS was assumed to be small also recognized the need for user selection under zero-forcing (ZF) [52] and BD [35] precoding but they only considered the downlink, and did not impose minimum rate requirements for users nor explore the impact different group sizes have on achieving minimum rates.

Some earlier work also studied how to jointly provide DL and UL QoS guarantees in TDD-based systems. [53] examined the problem of dynamic resource sharing in TDD OFDMA networks with symmetric DL and UL MBR requirements; and [54] studied the problem of providing minimum DL and UL SINR levels to users in a multi-cell TDD-LTE system where cells may have different time-slot configurations. However, neither of these papers incorporated MIMO into their systems.

Main takeaway of our literature review:

To the best of our knowledge, no previous work has examined the problem of planning a network while optimizing the resource configuration and user selection to jointly provide a minimum data rate for the DL and UL in an OFDM-based MU-MIMO system. Through the application of user grouping, our problem is generalized to the case where $U > N$ (though it could just as easily be applied when $U \leq N$). We believe that our analysis of the optimal user group configuration and TDD configuration to jointly dimension the DL and UL is a novel approach to this type of problem.

3.3 System Model and RRM Processes

We consider a DL and UL MU-MIMO system, with a BS having M_{BS} antennas and a certain number of homes each having M_{H} antennas. The system is TDD. A frame is composed of T slots in the time-domain, T_d allocated to the DL and T_u allocated to the UL ($T_d + T_u = T$). In the frequency domain the system has a bandwidth B made up of a total of C subchannels, each with bandwidth B_C. A PRB is composed of one subchannel and one time-slot, and, hence, there are $C \times T$ PRBs in a frame. The BS transmits with power $P_{\max}$ on the DL and each FWA home transmits with power P_{H} on the UL. On the DL, the power budget is shared equally by the PRBs in a given time-slot, i.e., $P^d_{PRB} = \frac{P_{\max}}{C}$. On the UL, the power allocated to a PRB by home k is $P^k_{PRB} = \frac{P_{\text{H}}}{C_k}$ where $C_k \leq C$ is the number of channels allocated to home k (to be detailed later). Because we are considering a rural environment with little to no inter-cell interference, we adopt a single-cell circular topology with a radius $\mathcal{R}$. In the following we refer to

$$\mathcal{S} = (B, C, P_{\max}, P_{\text{H}}, MBR_d, MBR_u, M_{\text{BS}}, M_{\text{H}})$$

as the system *setting*. Next, we describe the different RRM processes.

3.3.1 User Selection

For a given setting $\mathcal{S}$, a radius $\mathcal{R}$, a given realization $\omega(U)$ (which is characterized by a randomly distributed set of U FWA homes and their channel matrices as discussed later), user selection is performed once and for all at the beginning. We adopt a grouping strategy that divides homes into equal-sized groups of $S \leq N$ homes (let S_u (resp. S_d) be the group size on the UL (resp. DL)). Note that grouping is done separately for the UL and DL and hence S_u and S_d might be different. In this chapter, we adopt a random strategy when grouping homes. Smarter grouping strategies, for example, ones which consider the location of homes relative to one another, are for further study.

In the following we refer to the triple

$$\mathcal{V} = (T_u, S_d, S_u)$$

as the system *configuration* and the pair $\mathcal{V}_d = (T_u, S_d)$ (resp. $\mathcal{V}_u = (T_u, S_u)$) as the DL (resp. UL) system configuration. The outcome of the user selection process for a configuration $\mathcal{V}$ and a realization $\omega(U)$, is the creation of static groups of homes.

For a given system setting $\mathcal{S}$ and a radius $\mathcal{R}$, we consider a large set $\Omega(U)$ of realizations with U homes. If more than 95% of the realizations can offer (at least) MBR_d and MBR_u

to their U homes with configuration $\mathcal{V}$, we say that the configuration $\mathcal{V}$ is U-feasible. Note that there might be many feasible configurations for U for a setting $\mathcal{S}$ and a radius $\mathcal{R}$.

3.3.2 Channel Allocation

From above, the user selection process divides the homes in the realization $\omega(U)$ into static groups of size S_d in the DL and S_u in the UL. In the DL there is a total of $G(S_d) = \left\lceil \frac{U}{S_d} \right\rceil$ groups $\hat{\mathcal{U}}_1, \ldots, \hat{\mathcal{U}}_{G(S_d)}$, and each group $\hat{\mathcal{U}}$ is randomly assigned a set $\mathcal{C}_d(\hat{\mathcal{U}})$ of $n(S_d) = \left\lfloor \frac{C}{G(S_d)} \right\rfloor$ subchannels (note that there might be $n' < n(S_d)$ leftover subchannels, in which case one extra subchannel is given to the first n' groups). For the UL there is a total of $G(S_u) = \left\lceil \frac{U}{S_u} \right\rceil$ groups $\hat{\mathcal{U}}_1, \ldots, \hat{\mathcal{U}}_{G(S_u)}$, each of which is randomly assigned a set $\mathcal{C}_u(\hat{\mathcal{U}})$ of $n(S_u) = \left\lfloor \frac{C}{G(S_u)} \right\rfloor$ subchannels. Note that both user selection and channel allocation are static, i.e., they do not change from one frame to another.

3.3.3 Precoding and Combining Schemes

Given a setting $\mathcal{S}$, a radius $\mathcal{R}$, a configuration $\mathcal{V}$, and a realization $\omega(U)$, we perform precoding and combining for each distinct group of homes, created during user selection and its channels independently for the UL and DL once at the start of each frame. Note that the maximum number of streams at each home is M_{H}. At this stage, we assume that there are $L = M_{\mathrm{H}}$ streams per home. However, through PD, we might not allocate enough power to some streams to have a non-zero rate in some PRBs (see Section 3.4).

Full channel state information (CSI) is assumed to be known at the serving cell. We represent the channel matrix between the BS and the k-th home at PRB (c, t) as $\mathbf{G}_k^{c,t} = \mathbf{G}_k^c$. Since each home is fixed, the channel coherence time is large; hence, we assume that the channel coefficients are constant throughout a frame. On the other hand, we do not assume the channel is flat in frequency (i.e., it is frequency-selective). Furthermore, we assume that the channel is the same in the DL and UL because the system is TDD. Note that the channel model itself does not impact the system model and problem formulation. Hence, we leave the details of the channel model to Section 3.5 where we present the numerical settings and results.

We adopt a normalized BD precoding and combining process, which enables us to decouple precoding and combining (a computation that does not require any optimization) from power distribution. Furthermore, since we assume equal power allocation for each

subchannel, we may perform precoding and combining independently per PRB. Since, subchannels are time-invariant within a frame and a subchannel is allocated to the same group within a frame, we only need to perform precoding/combining once per subchannel per frame. Hence, given a group of $\hat{U} \leq N$ homes, denoted by $\hat{\mathcal{U}}$, is selected for a subchannel c in a frame, under BD, the normalized precoding matrix at the BS in subchannel c given by $\mathbf{W}_k^c = \left[\mathbf{w}_{k,1}^c, \ldots, \mathbf{w}_{k,L}^c\right] \in \mathbb{C}^{M_{\text{BS}} \times L}$ is used to transmit data symbols to each stream $l \in \{1, 2, \ldots, L\}$, and the combining matrix at each home given by $\mathbf{U}_k^c = \left[\mathbf{u}_{k,1}^c, \ldots, \mathbf{u}_{k,L}^c\right]^T \in \mathbb{C}^{L \times M_{\text{H}}}$ is used to recover the data symbols. More details about BD can be found in [35, 44–46].

The output of the normalized precoding and combining process is a set of effective channels for each (possible) user stream. We then input these effective channels into our PD problem formulation, which performs power distribution (and indirectly stream selection) to verify if the configuration $\mathcal{V}$ is feasible for $\omega(U)$, i.e., if all homes in the realization can be offered the MBRs. Note that we determine the effective channels for all L streams even though less streams could be selected via PD.

Next, we outline the steps needed to compute the effective channels for a single subchannel on the DL for a given group of homes $\hat{\mathcal{U}}$. For brevity, we omit the per-subchannel superscript c in the following. Due to symmetry in the channel, the UL procedure is the same as the DL procedure, except that the precoding matrix at the BS in the DL becomes the combining matrix at the BS in the UL and the combining matrix at the home in the DL becomes the precoding matrix at the home in the UL. The resulting effective channels are the same for the UL and DL.

Let $\mathbf{s}_k = [s_{k,1}, s_{k,2}, \ldots, s_{k,L}] \in \mathbb{C}^{L \times 1}$ be the dedicated data symbol vector for the k-th home, where $s_{k,l}$ is the data symbol for stream l, $\mathbb{E}\{\mathbf{s}_k \mathbf{s}_k^H\} = \mathbf{I}_L$, $k \in \hat{\mathcal{U}}$ and $\mathbf{I}_L$ is the $L \times L$ identity matrix. The recovered data symbols at each home are given by

$$\hat{\mathbf{s}}_k = \mathbf{U}_k \mathbf{G}_k \mathbf{W}_k \mathbf{P}_k \mathbf{s}_k + \underbrace{\sum_{i \in \hat{\mathcal{U}}, i \neq k} \mathbf{U}_k \mathbf{G}_k \mathbf{W}_i \mathbf{P}_i \mathbf{s}_i}_{\text{inter-user interference}} + \mathbf{U}_k \mathbf{z}_k, \quad k \in \hat{\mathcal{U}}, \tag{3.1}$$

where $\mathbf{G}_k = \left[\mathbf{g}_k^1, \ldots, \mathbf{g}_k^{M_{\text{H}}}\right]^T \in \mathbb{C}^{M_{\text{H}} \times M_{\text{BS}}}$ is the channel matrix between the BS and home, $\mathbf{P}_k \in \mathbb{R}_+^{L \times L}$ is a diagonal matrix representing the power distribution for the data streams of the k-th home, and $\mathbf{z}_k \sim \mathcal{CN}(0, \sigma^2 \cdot \mathbf{I}_{M_{\text{H}}})$ is the additive white Gaussian noise (AWGN).

The key idea behind BD precoding is to select the precoding matrix to fully suppress the inter-user interference, i.e.,

$$\mathbf{G}_k \mathbf{W}_i \mathbf{P}_i = \mathbf{0}, \quad \forall i, k \in \hat{\mathcal{U}}, i \neq k. \tag{3.2}$$

To do so, let $\widetilde{\mathbf{G}}_k$ represent the channel matrix from the BS to all homes except the k-th home, i.e., $\widetilde{\mathbf{G}}_k = [\mathbf{G}_1^T, \ldots, \mathbf{G}_{k-1}^T, \mathbf{G}_{k+1}^T, \ldots, \mathbf{G}_{\hat{U}}^T]^T$. By conducting singular value decomposition (SVD) for $\widetilde{\mathbf{G}}_k$, we have

$$\widetilde{\mathbf{G}}_k = \widetilde{\mathbf{T}}_k \widetilde{\mathbf{\Lambda}}_k [\widetilde{\mathbf{V}}_k^1 \quad \widetilde{\mathbf{V}}_k^0]^H, \quad k \in \hat{\mathcal{U}}, \tag{3.3}$$

where $\widetilde{\mathbf{T}}_k \in \mathbb{C}^{(\hat{U}-1)M_{\mathrm{H}} \times (\hat{U}-1)M_{\mathrm{H}}}$ is a unitary matrix; $\widetilde{\mathbf{\Lambda}}_k \in \mathbb{R}_+^{(\hat{U}-1)M_{\mathrm{H}} \times M_{\mathrm{BS}}}$ a rectangular diagonal matrix; $\widetilde{\mathbf{V}}_k^1 \in \mathbb{C}^{M_{\mathrm{BS}} \times (M_{\mathrm{BS}} - R_k)}$ and $\widetilde{\mathbf{V}}_k^0 \in \mathbb{C}^{M_{\mathrm{BS}} \times R_k}$ are the submatrices composed of the right-singular vectors corresponding to non-zero and zero singular values, respectively, where $R_k > 0$ is the dimension of the nullspace of $\widetilde{\mathbf{G}}_k$. (In order to have zero inter-user interference, $\mathbf{W}_k \mathbf{P}_k$ must lie in the nullspace of $\widetilde{\mathbf{G}}_k$; hence, the null space of $\widetilde{\mathbf{G}}_k$ must have a dimension that is greater than 0.) From this, we obtain the non-interfering block effective channel matrix

$$\mathbf{G}_k^e = \mathbf{G}_k \cdot \widetilde{\mathbf{V}}_k^0, \quad k \in \hat{\mathcal{U}} \tag{3.4}$$

Through (3.4), the MU-MIMO system reduces into $\hat{U}$ parallel and non-interfering single-user MIMO (SU-MIMO) systems. From this, we can separately derive the (normalized) precoding and combining per user stream (k, l). To do so, we perform SVD on the effective channel matrix (3.4) for every home k [46]

$$\mathbf{G}_k^e = \mathbf{T}_k^e \cdot \mathbf{\Lambda}_k^e \cdot (\mathbf{V}_k^e)^H, \quad k \in \hat{\mathcal{U}}, \tag{3.5}$$

where $\mathbf{T}_k^e \in \mathbb{C}^{M_{\mathrm{H}} \times M_{\mathrm{H}}}$ and $\mathbf{V}_k^e \in \mathbb{C}^{R_k \times R_k}$ are unitary matrices, and $\mathbf{\Lambda}_k^e \in \mathbb{R}_+^{M_{\mathrm{H}} \times R_k}$ is a rectangular diagonal matrix containing singular values of $\mathbf{G}_k^e$ and its elements are sorted in descending order

$$\mathbf{\Lambda}_k^e = \begin{bmatrix} \lambda_{k,1} & \cdots & & \mathbf{0} \\ & \ddots & & \\ \mathbf{0} & \cdots & \lambda_{k,L} & \mathbf{0} \end{bmatrix} \tag{3.6}$$

where $\lambda_{k,l} = |\mathbf{u}_{k,l} \mathbf{G}_k \mathbf{w}_{k,l}|$ is the normalized precoding and combining on stream (k, l). Thus, the effective channel for stream $l \in \{1, \ldots, L\}$ of home $k \in \hat{\mathcal{U}}$ is

$$E_{k,l} = \frac{\lambda_{k,l}^2}{\sigma^2}. \tag{3.7}$$

Recall that there is an effective channel per stream per home in the group, per subchannel allocated to that group.

3.3.4 Power Distribution

Given a setting $\mathcal{S}$, a radius $\mathcal{R}$, a configuration $\mathcal{V}$, a direction (either UL or DL), a realization $\omega(U)$, a grouping of homes obtained via user selection and their channel, and the per stream effective channels for each home in the groups, our next challenge is to verify if the configuration is feasible, i.e., if there exists a per stream PD that enables each selected home to receive its MBR in each direction. At this stage a stream that does not receive enough power to see a non-zero rate in a PRB can be considered as not being selected; hence, even though we had set L to its maximum value M_{H} initially, PD might give a home less streams. We cast this PD problem as a max-min problem as presented in Section 3.4.

The outcome of PD is the power per PRB per stream per home. With these powers, the SINR for each stream of each home in each PRB can be computed.

3.3.5 Rate Computation Using Modulation and Coding Scheme

A modulation and coding scheme defines the spectral-efficiency function which maps the SINR to a spectral efficiency. In contrast to most of the earlier papers providing MBRs that utilize the Shannon capacity [38,40,41,47,49–51,53], we use a practical MCS function which is piece-wise constant and characterized by Q pairs (SE_q, S_q), i.e., if $S_q \leq SINR_{k,l}^{c,t} < S_{q+1}$, then the spectral efficiency seen by the l-th data stream is SE_q (where $S_1 < S_2 < \cdots$ and $\mathrm{SE}_1 < \mathrm{SE}_2 < \cdots$).

The outcome of this process is the rate seen by each home in each PRB, i.e., the sum of the rates seen by each stream of that home in that PRB.

3.4 PD Problems Formulation and User Limit Computations

In this section, we focus on the power distribution problems as well as the procedure to compute the user limit. These steps are called after user selection (i.e., grouping), channel allocation and precoding and combining are performed. Recall that the UL and DL PD problems can be decoupled by fixing the number of slots T_u allocated to the UL and $T_d = T - T_u$ allocated to the DL. In determining the UL and DL user limits for all possible values of T_u, we will determine the optimal T_u (the value which maximizes the minimum of the UL and DL limit).

We work with a full buffer assumption. In other words, we assume that each of the homes is greedy and there is an infinite supply of bits at the cell to be sent to the homes in the DL and an infinite supply of bits at the homes to be sent to the BS in the UL. The full buffer assumption enables us to work with rates without needing to consider short-term traffic fluctuations that could otherwise cause the buffer to be empty or insufficiently full to meet the MBR in a given frame. This model works well in a planning stage for understanding the achievable user limit for a given system setting and a given radius and the configuration required to achieve that limit. We will first formulate the problem for the DL; next, we will formulate the UL problem; and then we will explain how to obtain the user limits.

3.4.1 Downlink Formulation

For a given setting and radius, for a given realization $\omega(U)$, a given DL configuration $\mathcal{V}_d = (T_u, S_d)$, the downlink user selection (i.e., user grouping) process divides the homes into static groups of size S_d. There is a total of $G(S_d) = \left\lceil \frac{U}{S_d} \right\rceil$ groups $\hat{\mathcal{U}}_1, \ldots, \hat{\mathcal{U}}_{G(S_d)}$[2], and each group $\hat{\mathcal{U}}$ is randomly assigned a set $\mathcal{C}_d(\hat{\mathcal{U}})$ of $n(S_d) = \left\lfloor \frac{C}{G(S_d)} \right\rfloor$ subchannels throughout the frame (note that there might be $n' < n(S_d)$ leftover subchannels, in which case one extra subchannel is given to the first n' groups). Given $L \leq M_{\mathrm{H}}$ streams per home, the per-stream effective channels are computed for each home in the group and for each subchannel in $\mathcal{C}_d(\hat{\mathcal{U}})$. The reason why we might choose $L < M_{\mathrm{H}}$ is because we might be interested in forcing the number of streams to be small to see the impact they have on performance. This is what we do in Section 3.5.2.

Given the downlink piecewise constant MCS function with a set of $\mathcal{Q}$ levels, $\mathcal{V}_d$, a group $\hat{\mathcal{U}}$ and its allocated subchannels $\mathcal{C}_d(\hat{\mathcal{U}})$, knowing the effective channels $\{E^c_{k,l}\}$, $k \in \hat{\mathcal{U}}$, $l \in \{1, \ldots, L\}$, $c \in \mathcal{C}_d(\hat{\mathcal{U}})$, the objective is to verify whether there exists a distribution of power $(P^{c,t}_{k,l})$ to each user stream in each PRB corresponding to channels in $\mathcal{C}_d(\hat{\mathcal{U}})$ so that we can give MBR_d to the homes in $\hat{\mathcal{U}}$. Let $\mathcal{T}_d$ be the set of DL time-slots, where $|\mathcal{T}_d| = T_d = T - T_u$. We formulate the problem $\mathbf{P^0_d}(\hat{\mathcal{U}}, \mathcal{V}_d, L)$ in a given frame as:

[2]Possibly some of the groups could have $S_d - 1$ homes instead of S_d.

$$\max_{\lambda(\hat{\mathcal{U}},\mathcal{V}_d,L),(P^{c,t}_{k,l}),(r^{c,t}_{k,l}),(\lambda_k),(I^{c,t}_{k,l,q})} \lambda(\hat{\mathcal{U}},\mathcal{V}_d,L) \tag{3.8}$$

$$\lambda_k \geq \lambda(\hat{\mathcal{U}},\mathcal{V}_d,L) \quad \forall k \in \hat{\mathcal{U}} \tag{3.9}$$

$$\lambda_k = \frac{1}{T} \sum_{c\in\mathcal{C}_d(\hat{\mathcal{U}})} \sum_{t\in\mathcal{T}_d} \sum_{l=1}^{L} r^{c,t}_{k,l} \quad \forall k \in \hat{\mathcal{U}} \tag{3.10}$$

$$\sum_{k\in\hat{\mathcal{U}}} \sum_{l=1}^{L} P^{c,t}_{k,l} \leq P^{d}_{PRB} = \frac{P_{\max}}{C} \quad \forall c \in \mathcal{C}_d(\hat{\mathcal{U}}), t \in \mathcal{T}_d \tag{3.11}$$

$$S_q I^{c,t}_{k,l,q} \leq P^{c,t}_{k,l} E^{c}_{k,l} \quad \forall c,t,k,l \in \{1,\dots,L\}, q \in \mathcal{Q} \tag{3.12}$$

$$r^{c,t}_{k,l} = B_C \sum_{q\in\mathcal{Q}} \mathrm{SE}_q I^{c,t}_{k,l,q} \quad \forall c,t,k,l \tag{3.13}$$

$$\sum_{q\in\mathcal{Q}} I^{c,t}_{k,l,q} \leq 1 \quad \forall c,t,k,l \tag{3.14}$$

$$I^{c,t}_{k,l,q} \in \{0,1\} \quad \forall c,t,k,l,q \tag{3.15}$$

Through (3.8) and (3.9), we seek to maximize the minimum user rate in the group $\lambda(\hat{\mathcal{U}},\mathcal{V}_d,L)$. (3.10) defines the rate λ_k given to home k in the frame, which is a function of the per-PRB, per-stream rates $r^{c,t}_{k,l}$. This problem uses the practical MCS function, where the selected MCS level q is determined by (3.12) and the resulting rate $r^{c,t}_{k,l}$ is given in (3.13). The per-PRB power P^{d}_{PRB} constrains the PD of the BS transmit power $P_{\max}/C$ allocated across every user stream in PRB (c,t) (see (3.11)). The practical MCS introduces integer variables $I^{c,t}_{k,l,q}$ (see (3.15)), making the problem a MINLP, which is difficult to solve.

To make the problem more tractable, we approximate the MCS function with a continuous function. Specifically, the rate given to the l-th stream of home k in PRB (c,t) can be approximated by [55]

$$r^{c,t}_{k,l} = B_C \min(SE_{\max}, a(SINR^{c,t}_{k,l})^b) \tag{3.16}$$

where $a > 0$, $0 \leq b \leq 1$, $SE_{\max}$ is the highest SE of the practical MCS function and $SINR^{c,t}_{k,l} = P^{c,t}_{k,l} E^{c}_{k,l}$. We denote $r_{max} = B_C SE_{\max}$ in the following. Note that this function is continuous and gives a non-zero rate for any $SINR > 0$ while the practical MCS function is strictly positive only if $SINR \geq S_1$ where S_1 is the first threshold of the MCS function.

With (3.16), $\mathbf{P_d^0}(\hat{\mathcal{U}}, \mathcal{V}_d, L)$ can be approximated by $\mathbf{P_d}(\hat{\mathcal{U}}, \mathcal{V}_d, L)$:

$$\max_{\lambda(\hat{\mathcal{U}},\mathcal{V}_d,L),(P_{k,l}^{c,t}),(r_{k,l}^{c,t}),(\lambda_k)} \lambda(\hat{\mathcal{U}}, \mathcal{V}_d, L) \tag{3.17}$$

$$\lambda_k \geq \lambda(\hat{\mathcal{U}}, \mathcal{V}_d, L) \quad \forall k \in \hat{\mathcal{U}} \tag{3.18}$$

$$\lambda_k = \frac{1}{T} \sum_{c \in \mathcal{C}_d(\hat{\mathcal{U}})} \sum_{t \in \mathcal{T}_d} \sum_{l=1}^{L} r_{k,l}^{c,t} \quad \forall k \in \hat{\mathcal{U}} \tag{3.19}$$

$$\sum_{k \in \hat{\mathcal{U}}} \sum_{l=1}^{L} P_{k,l}^{c,t} \leq P_{PRB}^{d} = \frac{P_{\max}}{C} \quad \forall c \in \mathcal{C}_d(\hat{\mathcal{U}}), t \in \mathcal{T}_d \tag{3.20}$$

$$r_{k,l}^{c,t} \leq r_{max} \quad \forall c, t, k, l \in \{1, \ldots, L\} \tag{3.21}$$

$$r_{k,l}^{c,t} \leq B_C a (P_{k,l}^{c,t} E_{k,l}^{c})^b \quad \forall c, t, k, l \tag{3.22}$$

$\mathbf{P_d}$ is a NLP, which can be solved relatively easily offline, which is sufficient for planning purposes.

For a given realization $\omega(U)$, a given L, and a configuration $\mathcal{V}_d$ we solve $\mathbf{P}_d(\hat{\mathcal{U}}, \mathcal{V}_d, L)$ for every $\hat{\mathcal{U}} \subseteq \{\hat{\mathcal{U}}_1, \ldots, \hat{\mathcal{U}}_{G(S_d)}\}$. This computation uses the approximated MCS function (3.16). After determining the optimal powers $\{P_{k,l}^{c,t}\}$ we compute the per-stream SINRs for all the streams in each home in the group $\hat{\mathcal{U}}$ for each PRB corresponding to subchannels in $\mathcal{C}_d(\hat{\mathcal{U}})$, i.e., $SINR_{k,l}^{c,t} = P_{k,l}^{c,t} E_{k,l}^{c}$ and map the result through the practical 3GPP MCS function to determine the real rate $\bar{r}_{k,l}^{c,t}$ assigned to each user stream in each PRB. Note that if $SINR_{k,l}^{c,t} < S_1$, then stream l of home k receives a zero rate in PRB (c, t), which is equivalent to not selecting stream l in that PRB. The real DL rate given to each home in $\hat{\mathcal{U}}$ in the frame is

$$\bar{\lambda}_k = \frac{1}{T} \sum_{c \in \mathcal{C}_d(\hat{\mathcal{U}})} \sum_{t \in \mathcal{T}_d} \sum_{l=1}^{M_{\mathrm{H}}} \bar{r}_{k,l}^{c,t} \quad \forall k \in \hat{\mathcal{U}}. \tag{3.23}$$

If $\bar{\lambda}_k \geq MBR_d$ for all $k \in \hat{\mathcal{U}}$ then $(\mathcal{V}_d, L)$ is feasible for group $\hat{\mathcal{U}}$ of the realization $\omega(U)$ on the DL. If $(\mathcal{V}_d, L)$ is feasible for all $\hat{\mathcal{U}} \subseteq \{\hat{\mathcal{U}}_1, \ldots, \hat{\mathcal{U}}_{G(S_d)}\}$, we say that $(\mathcal{V}_d, L)$ is feasible for realization $\omega(U)$ on the DL.

As mentioned earlier, for a given system setting $\mathcal{S}$, we consider a large set $\Omega(U)$ of realizations with U homes. If there exists a pair $(\mathcal{V}_d, L)$ for which 95% of the realizations are feasible, then we say that $(\mathcal{V}_d, L)$ is U-feasible on the DL. As also noted earlier, there could be many feasible such pairs, which could have an impact on the way the system is operated as discussed in Section 3.5.4.

3.4.2 Uplink formulation

For a given setting and radius, for a given realization $\omega(U)$, an uplink configuration $\mathcal{V}_u = (T_u, S_u)$, the uplink user selection (i.e., user grouping) process divides the homes into static groups of size S_u. There is a total of $G(S_u) = \left\lceil \frac{U}{S_u} \right\rceil$ groups $\hat{\mathcal{U}}_1, \ldots, \hat{\mathcal{U}}_{G(S_u)}$, and each group $\hat{\mathcal{U}}$ is randomly assigned a set $\mathcal{C}_u(\hat{\mathcal{U}})$ of $n(S_u) = \left\lfloor \frac{C}{G(S_u)} \right\rfloor$ subchannels throughout the frame. Given $L \leq M_{\mathrm{H}}$ streams per home, the per-stream effective channels are computed for each home in the group and for each subchannel in $\mathcal{C}_u(\hat{\mathcal{U}})$.

Given the uplink piecewise constant MCS function with a set of $\mathcal{Q}$ levels (which might not be the same as the MCS function on the DL), $\mathcal{V}_u$, a group $\hat{\mathcal{U}}$ and its allocated subchannels $\mathcal{C}_u(\hat{\mathcal{U}})$, knowing the effective channels $\{E^c_{k,l}\}$, $k \in \hat{\mathcal{U}}$, $l \in \{1, \ldots, L\}$, $c \in \mathcal{C}_u(\hat{\mathcal{U}})$, the objective is to verify whether there exists a distribution of power $(P^{c,t}_{k,l})$ to each user stream in each PRB corresponding to channels in $\mathcal{C}_u(\hat{\mathcal{U}})$ so that we can give MBR_u to all the homes in $\hat{\mathcal{U}}$. Let $\mathcal{T}_u$ be the set of UL time-slots, where $|\mathcal{T}_u| = T_u$. We directly formulate the following approximated problem $\mathbf{P_u}(\hat{\mathcal{U}}, \mathcal{V}_u, L)$ on the UL (similar to $\mathbf{P_d}(\hat{\mathcal{U}}, \mathcal{V}_d, L)$ on the DL) as:

$$\max_{\lambda'(\hat{\mathcal{U}},\mathcal{V}_u,L),(P^{c,t}_{k,l}),(r^{c,t}_{k,l}),(\lambda'_k)} \lambda'(\hat{\mathcal{U}}, \mathcal{V}_u, L) \tag{3.24}$$

$$\lambda'_k \geq \lambda'(\hat{\mathcal{U}}, \mathcal{V}_u, L) \quad \forall k \in \hat{\mathcal{U}} \tag{3.25}$$

$$\lambda'_k = \frac{1}{T} \sum_{c \in \mathcal{C}_u(\hat{\mathcal{U}})} \sum_{t \in \mathcal{T}_u} \sum_{l=1}^{L} r^{c,t}_{k,l} \quad \forall k \in \hat{\mathcal{U}} \tag{3.26}$$

$$\sum_{l=1}^{L} P^{c,t}_{k,l} \leq P^k_{PRB} = \frac{P_{\mathrm{H}}}{|\mathcal{C}_u(\hat{\mathcal{U}})|} \quad \forall c \in \mathcal{C}_u(\hat{\mathcal{U}}), t \in \mathcal{T}_u, k \tag{3.27}$$

$$r^{c,t}_{k,l} \leq r_{max} \quad \forall c, t, k, l \tag{3.28}$$

$$r^{c,t}_{k,l} \leq B_C a (P^{c,t}_{k,l} E^c_{k,l})^b \quad \forall c, t, k, l \tag{3.29}$$

The key difference in the UL problem is seen in (3.27) where each home has its own power budget to distribute, instead of the power budget of the BS in the DL that has to be shared among all homes in the group in (3.20). The home power budget P_{H} of a home only needs to be shared among $\mathcal{C}_u(\hat{\mathcal{U}})$, the subchannels allocated to its group.

We define in a similar fashion for the set of realizations $\Omega(U)$, the notion of U-feasibility on the uplink for a pair $(\mathcal{V}_u, L)$.

Finally, we say that a pair $(\mathcal{V}, L)$ is U-feasible for the system if $(\mathcal{V}_d, L)$ is U-feasible on the DL *and* $(\mathcal{V}_u, L)$ is U-feasible on the UL.

3.4.3 Computing User Limits

We aim to compute the user limit U^* for a given setting $\mathcal{S}$ and a given radius $\mathcal{R}$. Let $\mathcal{F}(\mathcal{V}, L)$ be the set of U for which $(\mathcal{V}, L)$ is U-feasible, for the system then

$$U^* = \max_{T_u, S_d, S_u, L} \{U \in \mathcal{F}(\mathcal{V}, L)\}.$$

Computing U^* using brute force is very cumbersome since we need to solve, for increasing values of U, and many realizations, problems $\mathbf{P_d}(\hat{\mathcal{U}}, \mathcal{V}_d, L)$ and $\mathbf{P_u}(\hat{\mathcal{U}}, \mathcal{V}_u, L)$ for each quadruple (T_u, S_d, S_u, L) $(1 \leq T_u \leq T-1,\ 1 \leq S_d, S_u \leq N,\ 1 \leq L \leq M_{\mathrm{H}})$ for all groups created on the DL and the UL by the DL and UL user selection. We can stop when for a given value of U, no quadruple is U-feasible. However, the value of U^* might be large if the number C of subchannels in the system is large and the radius is not too large making this computation time-consuming.

Instead, we propose a much simpler way to compute U^*. For a given system setting $\mathcal{S}$, a configuration $\mathcal{V} = (T_u, S_d, S_u)$, L streams, we compute for the DL (resp. the UL), how many subchannels $n(\mathcal{V}_d, L)$ (resp. $n(\mathcal{V}_u, L)$) are needed to offer MBR_d on the DL (resp. MBR_u on the UL) to 95% of the realizations, made of S_d (resp. S_u) homes, in a set Ω_d (resp. Ω_u). Note that, since $S_d \leq N$ and $S_u \leq N$, the amount of computations is much lower than with the brute force approach.

Specifically, given a setting $\mathcal{S}$ characterized in particular by the total number of subchannels in the system C, a radius $\mathcal{R}$, to compute the number of subchannels $n(\mathcal{V}_d, L)$ (resp. $n(\mathcal{V}_u, L)$) for a given configuration $\mathcal{V}_d$ (resp. $\mathcal{V}_u$) and L streams, we generate a set Ω_d of realizations (aka groups) of size S_d for a given DL configuration (T_u, S_d) and a set Ω_u of realizations (aka groups) of size S_u for a given UL configuration (T_u, S_u) (they are not the same realizations because, in general, $S_d \neq S_u$, although $|\Omega_d| = |\Omega_u| = \Omega$).

Focusing on the DL, given a realization ω_d with S_d homes, we compute $n(\mathcal{V}_d, L, \omega_d)$ the minimum number of channels necessary to offer MBR_d to all S_d homes in ω_d given T_u timeslots are allocated to the UL using Algorithm 1. Note that for a given MBR, the number of subchannels given to a home can be no less than $C_{\min}(MBR) = \left\lceil \frac{MBR}{B_C LSE_{\max}} \right\rceil$, where SE_{max} is the highest SE of the practical MCS function, otherwise it is impossible to give the homes the MBR. Hence, to speed up the algorithm, we initialize it with $n = C_{\min}(MBR)$

in Line 1. There is a subtlety in Line 2 for the DL. Indeed, on the DL, we solve the PD problem with n subchannels allocated to the group but with $P^d_{PRB} = \frac{P_{\max}}{C}$ where C is the number of subchannels allocated to the original system; hence $n(\mathcal{V}_d, L)$ is a function of C.

For the UL, we also use Algorithm 1 but when we solve the problem with n subchannels, $P^k_{PRB} = \frac{P_{\mathrm{H}}}{n}$.

Having computed $n(\mathcal{V}_d, L)$ (resp. $n(\mathcal{V}_u, L)$), we can compute the number of homes that can receive MBR_d on the DL (resp. MBR_u on the UL) if the system has C subchannels, i.e.,

$$U_d(\mathcal{V}_d, L, C) = \left\lfloor \frac{C}{n(\mathcal{V}_d, L)} \right\rfloor S_d \tag{3.30}$$

$$U_u(\mathcal{V}_u, L, C) = \left\lfloor \frac{C}{n(\mathcal{V}_u, L)} \right\rfloor S_u \tag{3.31}$$

This is because, we can create independent groups of size S_d and S_u respectively and allocate to each group the number of subchannels needed. Note that the above equations are true because when we allocate subchannels to groups the power per PRB neither changes on the DL (we keep $P^d_{PRB} = \frac{P_{\max}}{C}$ irrespective of the value of S_d) nor does it change on the UL (by construction). (3.30) and (3.31) could be computed exhaustively for every quadruple (T_u, S_d, S_u, L), but more efficient techniques can be applied to reduce computations (e.g., if (T_u, S_d, L) is determined to be infeasible in the DL, then we know that $(\widetilde{T}_u, S_d, L)$ is infeasible in the DL for all $\widetilde{T}_u > T_u$).

A search on T_u for different S_d and S_u then determines the correct configuration of T_u, S_d, S_u required to maximize the number of homes in the system. Let $U^*(L, C)$ be the user limit where

$$U^*(L, C) = \max_{T_u, S_d, S_u} \{\min(U_d(\mathcal{V}_d, L, C), U_u(\mathcal{V}_u, L, C))\}. \tag{3.32}$$

Let the triple

$$\mathcal{V}^*(L, C) = (T^*_u(L, C), S^*_d(T^*_u, L, C), S^*_u(T^*_u, L, C))$$

yielding $U^*(L, C)$ be the *optimal configuration* for the system setting $\mathcal{S}$ with C subchannels when there are L streams per home.

Clearly this simplified process gives us an estimate of what we could find through brute force. If necessary, we could use this estimate as a starting point to initialize a search for the real limit. That being said, we believe that the granularity provided by the simplified process we developed is acceptable for the purpose of planning a network. The user limit that we obtain also depends on our grouping strategy. It is possible that

Algorithm 1 Compute $n(\mathcal{V}_{d/u}, L, \omega_{d/u})$

1: $n \leftarrow C_{\min}(MBR_{d/u}) = \left\lceil \frac{MBR_{d/u}}{B_C LSE_{\max}} \right\rceil$
2: Solve $\mathbf{P_{d/u}}(\omega_{d/u}, \mathcal{V}_{d/u}, L)$ with n subchannels
3: **if** all $S_{d/u}$ homes receive $MBR_{d/u}$ **then**
4: $\quad n(\mathcal{V}_{d/u}, L, \omega_{d/u}) \leftarrow n$
5: **else**
6: $\quad n \leftarrow n + 1$
7: $\quad$ **if** $n \leq C$ **then**
8: $\quad\quad$ Go to 2
9: $\quad$ **else**
10: $\quad\quad$ $\omega_{d/u}$ infeasible
11: $\quad$ **end if**
12: **end if**

a more sophisticated user selection could offer the MBRs to more homes if we were to reformulate the problem as a *joint* user selection and power distribution problem that was solved per-realization. However, this would make the problem more difficult to compute and it could only be solved through brute force. The strength of our approach is that it is simple and robust and provides very useful insights to MNOs during the planning phase.

3.5 Numerical Results

In this section we present the numerical results of our study. We begin by describing the channel settings. Next we conduct an initial study of the case when $U \leq N$ and all U homes are selected in each PRB, which informs us about the impact of multiple streams on performance as well as how we can implement user grouping. Then we study the network planning problem when $U > N$, determining the user limit and the optimal configuration of T_u, S_d, and S_u for a given system setting and radius. We end the section by providing some useful insights into how MNOs could operate FWA networks.

3.5.1 System and Channel Settings

We adopt the 3GPP rural macro (RMa) path loss model [56], but assume that the MNO installs the FWA antennas at each home, guaranteeing a LOS view between every home

Table 3.1: System Parameters for Numerical Results

Parameters	**Values**
Carrier frequency (f_c)	3.5 GHz
Cell radius ($\mathcal{R}$)	{1500,2000,3000,4000,5000,10000} m
System bandwidth (B)	{25,50} MHz
Number of sub-channels (C)	{65,133}
Subchannel bandwidth (B_C)	360 kHz
Number of time-slots per frame (T)	20
Time-slot duration (T_S)	0.5 ms
Maximum power of BS ($P_{\max}$)	{40,80} W
Maximum power of home (P_{H})	400 mW
Total antennas at BS (M_{BS})	{64,128}
Total antennas at home (M_{H})	{4,8}
Minimum bit-rate in DL (MBR_d)	{15,30} Mbps
Minimum bit-rate in UL (MBR_u)	{2.5,5} Mbps
Minimum distance between BS and home ($d_{2D}^{\min}$)	35 m
Effective antenna height at BS (h_{BS})	100 m
Effective antenna height at home (h_{H})	5 m
Adjacent antenna distance at BS (d_a^{BS})	0.5 λ
Adjacent antenna distance at home (d_a^{H})	0.2 m
BS channel correlation coefficient (φ_{BS})	0.4
Home channel correlation coefficient (φ_{H})	$\exp\{-d_a^{\mathrm{H}}/\lambda\}$
Noise power density (N_0)	–174 dBm/Hz
Noise figure (ζ)	9 dB
Rician factor (κ)	$\mathcal{N}(7, 4^2)$ dB

and the BS. The BS transmits using a mid-band carrier frequency $f_c = 3.5\,\mathrm{GHz}$. We consider NR numerology 1 [18], which utilizes subchannels of bandwidth $B_C = 360\,\mathrm{kHz}$ and time-slots of length $T_S = 0.5\,\mathrm{ms}$. The frame has a total of $T = 20$ time-slots. We will vary the number of slots allocated to the uplink T_u in order to determine the user limit for a given system setting $\mathcal{S}$. We consider system bandwidths of $B = 25\,\mathrm{MHz}$ and $B = 50\,\mathrm{MHz}$, which correspond to $C = 65$ and $C = 133$ subchannels, respectively[3] [6].

The BS is located at the center of the cell and the homes are uniformly distributed within a circle of radius $\mathcal{R}$ and a minimum distance of $d_{2D}^{\min} = 35\,\mathrm{m}$ from the BS. The BS

[3]Due to the use of guard bands, the total number of subchannels does not scale linearly with the bandwidth.

Table 3.2: Tapped-Delay Line and Power Delay Profile [56]

Tap number	1	2	3	4	5	6	7	8
Delay t_d (ns)	0	51.33	54.40	56.30	54.40	71.12	190.92	192.93
ϱ_d	0.9209	0.0244	0.0144	0.0097	0.0048	0.0053	0.0128	0.0077

Table 3.3: SINR-SE Mapping Used for Practical MCS

SINR (dB)	-6.5	-4	-2.6	-1	1	3	6.6	10	11.4	11.8	13	13.8	15.6	16.8	17.6
Spectral efficiency (bps/Hz)	0.14	0.22	0.36	0.56	0.82	1.10	1.38	1.78	2.25	2.55	3.10	3.64	4.22	4.78	5.18

antennas are at height $h_{\mathrm{BS}} = 100\,\mathrm{m}$ and the home antennas are at height $h_{\mathrm{H}} = 5\,\mathrm{m}$.

We will consider several settings $\mathcal{S}$, by varying the number of antennas at the BS M_{BS}, the number of antennas at each home M_{H}, the BS transmit power $P_{\max}$, the system bandwidth B (and hence, the total subchannels C), and the MBR in the DL MBR_d and UL MBR_u for different cell radii $\mathcal{R}$.

We summarize the parameters used in the numerical computations in Table 3.1. The system settings that we vary are shown in braces {}. Unless otherwise specified, we use the default values for the 3GPP RMa channel model found in [56].

Since each home is fixed, the channel coherence time is large; hence, we assume that the channel coefficients are constant throughout the frame. A tapped-delay-line channel model with D taps is adopted, where the channel matrix $\mathbf{G}_k^{c,t}$ from the BS to the k-th home at PRB (c,t) can be written with respect to the D channel taps as [57]:

$$\mathbf{G}_k^{c,t} = \mathbf{G}_k^{c} = \sum_{d=1}^{D} \overline{\mathbf{G}}_k[d] \exp\left(-j2\pi\tau_d c/C\right), \tag{3.33}$$

where $\overline{\mathbf{G}}_k[d]$ is the channel matrix of the d-th tap, which is constant throughout the frame and has a normalized delay of τ_d. Note that the delay of the d-th tap $t_d = \tau_d/B$, where B is the system bandwidth. In our system, we utilize an 8-tap channel model, where the value of t_d is given in Table 3.2 [56].

With a LOS component from the BS, the first channel tap of each home follows a Rician distribution, i.e.,

$$\overline{\mathbf{G}}_k[1] = \sqrt{\varrho_1 \beta_k}\left(\sqrt{\frac{1}{1+\kappa_k}}\mathbf{R}_{\mathrm{H}}^{\frac{1}{2}}\mathbf{H}_G[1]\mathbf{R}_{\mathrm{BS}}^{\frac{1}{2}} + \sqrt{\frac{\kappa_k}{1+\kappa_k}}\mathbf{H}_k\right), \tag{3.34}$$

where κ_k is the Rician factor and $\mathbf{H}_k \in \mathbb{C}^{M_{\mathrm{H}} \times M_{\mathrm{BS}}}$ represents the LOS component from the BS to the k-th home. β_k denotes the large-scale fading channel coefficient, involving the power attenuation and shadowing between the BS and the k-th home, which is determined from the 3GPP RMa 3D path loss model shown in Table 7.4.1-1 of [56]. $\mathbf{H}_G[d] \in \mathbb{C}^{M_{\mathrm{H}} \times M_{\mathrm{BS}}}$, $d = 1, 2, \ldots, D$, is a random matrix whose entries are zero-mean i.i.d complex Gaussian random variables with unit variance; and $\mathbf{R}_{\mathrm{H}}$ (resp. $\mathbf{R}_{\mathrm{BS}}$) is the correlation matrix at the home (resp. the BS) assumed to be the same for every home and to not change with time. ϱ_d represents the normalized power of the d-th tap, and its value is shown in Table 3.2. In terms of $\mathbf{H}_k$, the LOS component from the m-th antenna of the BS, located at $\mathbf{a}_m \in \mathbb{R}^3$, to the n-th antenna of the k-th home, located at $\mathbf{u}_k^n \in \mathbb{R}^3$, is given by

$$h_k^{m,n} = e^{2\pi j \|\mathbf{u}_k^n - \mathbf{a}_m\|/\lambda}, \tag{3.35}$$

where $\lambda = 3 \times 10^8 / f_c$ is the wavelength, and f_c is the carrier frequency. Note that a LOS component only exists in the first channel tap, and all other channel taps follow a Rayleigh distribution [56], i.e.,

$$\overline{\mathbf{G}}_k[d] = \sqrt{\varrho_d \beta_k}\mathbf{R}_{\mathrm{H}}^{\frac{1}{2}}\mathbf{H}_G[d]\mathbf{R}_{\mathrm{BS}}^{\frac{1}{2}}, \quad d = 2, 3, \ldots, D. \tag{3.36}$$

The BS and all homes are assumed to be equipped with uniform planar arrays (UPA) with omnidirectional antennas; thus at the BS (resp. homes) there are $\sqrt{M_{\mathrm{BS}}}$ (resp. $\sqrt{M_{\mathrm{H}}}$) antennas in both vertical and horizontal directions with identical spacing d_a^{BS} (resp. d_a^{H}). Following [55, 58, 59], we adopt the exponential correlation model, where the (i, j)-th entry $[\mathbf{R}]_{i,j}$ of the correlation matrix $\mathbf{R}$ is given by

$$[\mathbf{R}_{\mathrm{BS}}]_{i,j} = \varphi_{\mathrm{BS}}^{|v(i)-v(j)|+|h(i)-h(j)|}, \quad i, j = 1, 2, \ldots, M_{\mathrm{BS}}, \tag{3.37}$$

$$[\mathbf{R}_{\mathrm{H}}]_{i,j} = \varphi_{\mathrm{H}}^{|v(i)-v(j)|+|h(i)-h(j)|}, \quad i, j = 1, 2, \ldots, M_{\mathrm{H}}, \tag{3.38}$$

where $0 \leq \varphi_{\mathrm{BS}}, \varphi_{\mathrm{H}} \leq 1$ denote the correlation coefficients between adjacent antennas at the BS and between adjacent antennas at homes, respectively; $v(m)$ and $h(m)$ are the vertical and horizontal indexes of the m-th antenna of the UPA. For the BS we set $\varphi_{\mathrm{BS}} = 0.4$ [55]; for the homes, since the number of FWA antennas is assumed to be small, the antenna separation d_a^{H} is large relative to λ and we set $\varphi_{\mathrm{H}} = e^{-d_a^{\mathrm{H}}/\lambda}$ [60].

NR defines several MCS tables for the downlink and uplink [61], and the network and User Equipment can switch from one table to another depending on the radio conditions. In general, the relationship between the radio channel and the selected MCS is not standardized and is typically derived through system and/or link-level simulations [62, 63]. For

simplicity we use only one of the NR MCS tables in our system. The table we use supports up-to 64-QAM modulation and is the table that would typically be selected for average-to-poor channel conditions (i.e., for cell edge users in a rural environment). In NR this table can be used for the DL and the UL (in LTE it was only used for DL) so we use it for both. The corresponding SINR-SE mapping is shown in Table 3.3 [55, 64].

For the MCS approximation in (3.16) we follow the results derived in [55] to approximate Table 3.3 and set $a = 0.648$ and $b = 0.5$. Thus, the rate of the l-th stream of home k in PRB (c, t) is approximated by

$$r_{k,l}^{c,t} = B_C \min(SE_{\max}, 0.648(P_{k,l}^{c,t} E_{k,l}^{c})^{0.5}) \tag{3.39}$$

3.5.2 Understanding the Impact of Streams and Group Sizes

As a first step, we study the case where $U \leq N$ for $L \in \{1, \ldots, M_{\mathrm{H}}\}$ and all U homes are selected in each PRB, i.e., there is a single group of size U. This will provide insight into how user grouping should be performed when $U > N$ (basically, what we will show is that using $S_d = N = S_u$ is *not* the right thing to do when $U > N$). We will also observe the impact on the performance of limiting the number of streams to less than M_{H}.

In this first numerical section devoted to $U \leq N$, we set $B = 25\,\mathrm{MHz}$, $C = 65$ sub-channels, $M_{\mathrm{BS}} = 64$ antennas, $M_{\mathrm{H}} = 4$ antennas, $P_{\max} = 40\,\mathrm{W}$, $MBR_d = 30\,\mathrm{Mbps}$ and $MBR_u = 5\,\mathrm{Mbps}$, which we refer to as the *baseline* setting in the remainder of the chapter. We will study the impact of all the above parameters later. With $M_{\mathrm{BS}} = 64$ and $M_{\mathrm{H}} = 4$ we have $N = 16$; hence we examine the case where $U \leq 16$. Also, the maximum number of streams per home is $M_{\mathrm{H}} = 4$. We set $T_u = \frac{T}{2} = 10$ slots. Clearly, the results are very dependent on the value of T_u as will be discussed at the end of this section.

For every $U \leq N$, we generate $\Omega = 100$ realizations. Each realization $\omega(U)$ corresponds to a set $\mathcal{U}$ of U homes along with their channel matrices. We compute the effective channels assuming $L = M_{\mathrm{H}}$ streams are selected (recall that if $L < M_{\mathrm{H}}$ the effective channels for the existing streams will still be the same). For each $\omega(U)$ and each L we solve $\mathbf{P_d}(\mathcal{U}, \mathcal{V}_d, L)$ to obtain the power distribution that maximizes the minimum of the home rates, and verify using the real MCS function whether every home receives a rate of at least MBR_d. Likewise, we solve $\mathbf{P_u}(\mathcal{U}, \mathcal{V}_u, L)$ in the UL to confirm whether each home receives a rate of at least MBR_u.

In Figure 3.1, we plot the 95^{th} percentile of the minimum DL user rate (among the U homes) for different numbers of streams under the baseline system settings when the radius is $\mathcal{R} = 1500\,\mathrm{m}$ and $T_u = 10$ as a function of U. The results in Figures 3.1a, 3.1b

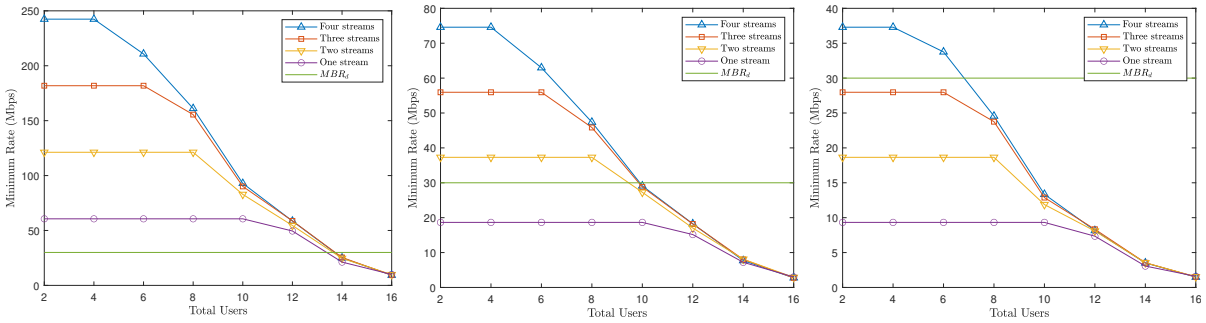

(a) 65 subchannels allocated per home.

(b) 20 subchannels allocated per home.

(c) 10 subchannels allocated per home.

Figure 3.1: 95^{th} percentile of minimum DL user rates for $U \leq N$: $\Omega = 100$, $\mathcal{R} = 1500\,\text{m}$, $B = 25\,\text{MHz}$, $M_{\text{BS}} = 64$, $M_{\text{H}} = 4$, $P_{\max} = 40\,\text{W}$, $MBR_d = 30\,\text{Mbps}$, $T_u = 10$. The power per PRB is $\frac{P_{\max}}{65}$ for all cases.

and 3.1c correspond to the cases where homes are allocated 65, 20, and 10 subchannels, respectively. For all cases the DL PRB power is fixed, i.e., $P^d_{PRB} = \frac{P_{\max}}{65}$. We observe that limiting the number of streams to less than M_{H} is impacting the performance a lot. Indeed, multiple streams can greatly improve the performance when U, the number of homes, is small relative to N. However, as U increases, we begin to see the curves for different numbers of streams overlapping, which indicates that PD is not selecting all streams, e.g., when $U = 8$, the fourth stream provides almost no benefit. On the other hand, the results also make it clear that for certain numbers of homes, using too few streams could greatly degrade performance, e.g., for $U < 10$, limiting the number of streams to one per home could degrade performance by a factor of 3 to 4. Therefore, it is clear that the appropriate number of streams is dependent on the selected number of homes. By using PD to perform stream selection, we can automatically determine that number.

Figure 3.1a also shows that with $MBR_d = 30$ Mbps and $T_u = 10$, we cannot guarantee MBR_d to every home for $U = 14$ or $U = 16$ even if they are allocated all the 65 subchannels. On the other hand, Figure 3.1b shows that with 20 subchannels we can give 8 homes MBR_d; hence, to give 16 homes MBR_d we could simply divide the homes into two groups and give each group 20 subchannels. Thus, we learn that for U close to N, it might be better to divide homes into groups and allocate a fraction of the subchannels to each group than to select all homes at once and give them all of the subchannels.

These results also illustrate how grouping can be used to serve $U > N$ homes. For example, continuing from above, after allocating 40 subchannels across the first two groups

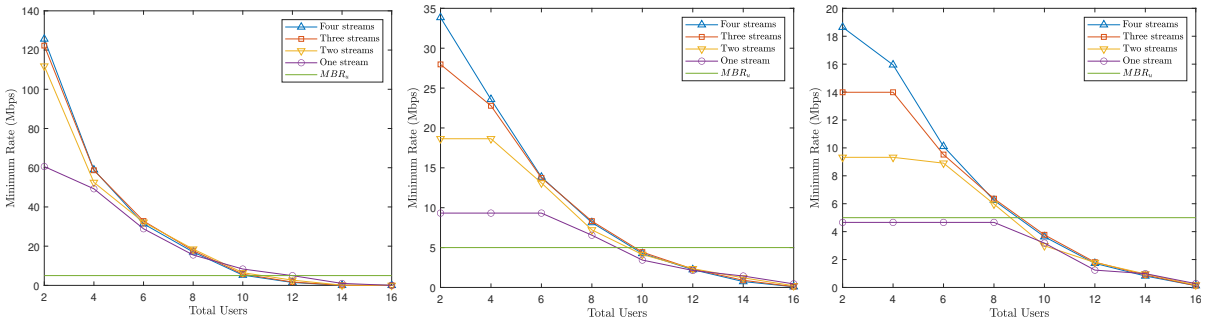

(a) 65 subchannels allocated per home.

(b) 10 subchannels allocated per home.

(c) 5 subchannels allocated per home.

Figure 3.2: 95^{th} percentile of minimum UL user rates for $U \leq N$: $\Omega = 100$, $\mathcal{R} = 1500\,\text{m}$, $B = 25\,\text{MHz}$, $M_{\text{BS}} = 64$, $M_{\text{H}} = 4$, $P_{\text{H}} = 400\,\text{mW}$, $MBR_u = 5\,\text{Mbps}$, $T_u = 10$.

of 8 homes, there would be 25 unallocated subchannels remaining. Hence an additional 8 homes could easily be given MBR_d for a total of 24 homes served. However, we are not limited to 24 homes: Figure 3.1c shows that with 10 subchannels, 6 homes can be given MBR_d; thus with 65 subchannels total, we could instead form 6 groups of 6 homes and give MBR_d to a total of 36 homes.

We plot in Figure 3.2, similar results for the UL for $U \leq N$ with the baseline settings when $\mathcal{R} = 1500\,\text{m}$ and $T_u = 10$. In this case we look at subchannel allocations of 65, 10 and 5 in Figures 3.2a, 3.2b and 3.2c, respectively. Recall from (3.27) that the UL power per PRB P^k_{PRB} is inversely proportional to the number of subchannels allocated to the home. As was the case for the DL, the UL also benefits from multiple streams when the number of homes is small.

For the UL, we also see that grouping is necessary to serve more than 10 homes, as we cannot select $U > 10$ home at once and give them all MBR_u even with 65 subchannels (Figure 3.2a). We could easily give 16 homes MBR_u by dividing them into two groups of 8 and giving each group 10 subchannels (Figure 3.2b), but we could also do the same with 5 subchannels per group (Figure 3.2c). The latter approach (5 subchannels) allows us to serve many more homes in the UL simultaneously. Taking groups of $S_u = 8$ homes and giving each group 5 subchannels would enable 104 homes to receive MBR_u. On the other hand, in the DL, there is no group size S_d with which we could allocate all 65 subchannels to the groups to give a total of 104 homes MBR_d (in fact, our computations have shown that the best we can do on the DL for $T_u = 10$ is to offer the MBR to 40 homes). Hence, for the baseline setting and $T_u = 10$, we see that the DL is the *bottleneck* of the system.

Setting	Parameters $\mathcal{S}$						
	M_{BS}	M_{H}	B (MHz)	C	$P_{\max}$ (W)	MBR_d (Mbps)	MBR_u (Mbps)
Baseline	64	4	25	65	40	30	5
Double bandwidth	64	4	**50**	**133**	**80**	30	5
Double BS antennas	**128**	4	25	65	40	30	5
Double home antennas	64	**8**	25	65	40	30	5
Double BS power	64	4	25	65	**80**	30	5
Half MBR	64	4	25	65	40	**15**	**2.5**

Table 3.4: System settings we consider. Parameters that differ from baseline are in bold.

Clearly, decreasing T_u would provide more resources to the DL, which would increase the number of homes that can receive MBR_d while the number of homes that can receive MBR_u would decrease. At a certain point, i.e., a certain value of T_u, the UL would become the bottleneck.

3.5.3 Network Planning Results

Now our goal is to determine, for a given system setting $\mathcal{S}$, the user limit $U^*(\mathcal{S})$ as well as a configuration $\mathcal{V}^*(\mathcal{S})$ that achieves that limit for a given radius. For this study we set $L = M_{\text{H}}$ and allow PD to perform stream selection. In addition to the baseline setting, we examine the impact from doubling the overall bandwidth B, doubling the number of antennas at the BS M_{BS}, doubling the number of antennas at the homes M_{H}, doubling the power at the BS $P_{\max}$, and halving MBR_d and MBR_u for different cell radii, i.e., $\mathcal{R} \in \{1500, 2000, 3000, 4000, 5000, 10000\}$ (meters). Note that when doubling the bandwidth the total BS power must also be doubled in order to maintain the same power per MHz. The different system settings are summarized in Table 3.4.

We initially study the baseline system for $|\Omega| = 100$ realizations. Using Algorithm 1, we compute the number of subchannels necessary to offer MBR_d and MBR_u for 95% of realizations for different group sizes and for $T_u \in [1, 19]$. Based on these results, we determine the DL and UL user limits for the baseline setting and $\mathcal{R} = 1500\,\text{m}$, which we plot in Figure 3.3 as a function of T_u. From the figure, we can see that the baseline setting is able to offer the MBR on the DL and UL to 60 homes (i.e., $U^* = 60$) when $\mathcal{R} = 1500\,\text{m}$. This happens when $T_u^* = 4$, i.e., only 20% of the time-slots are given to the UL. This result is achieved with the optimal group sizes $S_d^* = 6$ and $S_u^* = 4$ which are both much lower than $N = 16$.

Now we conduct the same study for $\mathcal{R} = 5000\,\text{m}$ (the other setting parameters are as

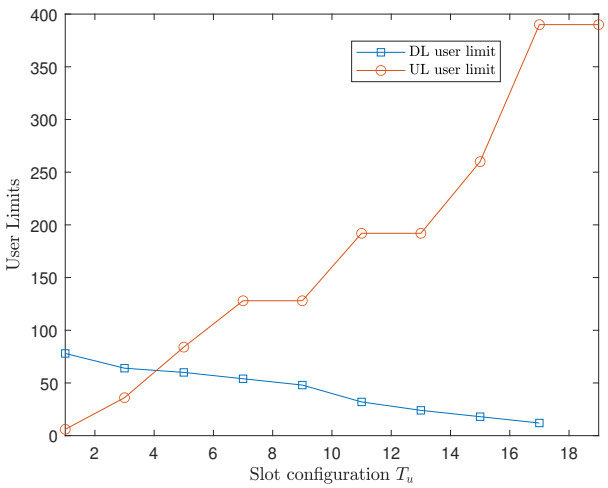

Figure 3.3: DL and UL user limits for different T_u: baseline setting with $\mathcal{R} = 1500\,\text{m}$.

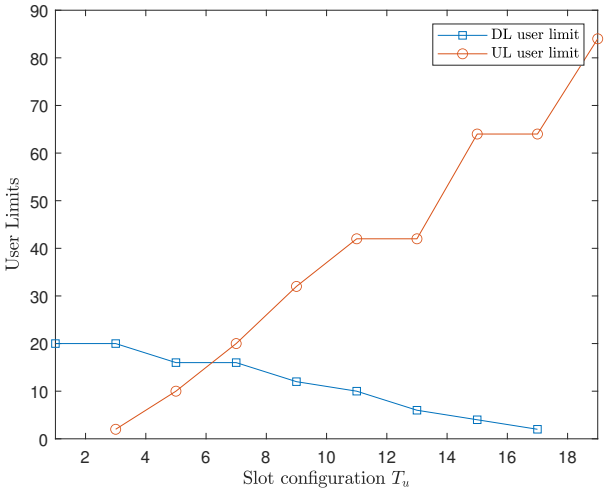

Figure 3.4: DL and UL user limits for different T_u: baseline setting with $\mathcal{R} = 5000\,\text{m}$.

$\mathcal{R}$	$U^*(\mathcal{R})$	$T_u^*(\mathcal{R})$	$S_d^*(\mathcal{R})$	$S_u^*(\mathcal{R})$
1500	60	4	6	4
2000	42	5	6	4
3000	32	5	4	4
4000	22	6	4	2
5000	15	6	4	2
10000	3	11	2	1

Table 3.5: User limits for the baseline setting and different radii, with corresponding slot configuration and group sizes required to attain limit.

per the baseline) and plot the results in Figure 3.4. We obtain $U^* = 15$, $T_u^* = 6$, which are achieved by $S_d^* = 4$, $S_u^* = 2$. Not surprisingly, the user limit is much lower (15) than the one (60) for the original radius of 1500 m and the optimal group sizes are quite small.

In Table 3.5, we summarize the user limits and the optimal configurations achieving these limits for the baseline setting for different cell radii. It is clear that the optimal configuration is dependent on the cell radius. Furthermore, the advantage of user grouping is clear: for $\mathcal{R} < 5000$ m the user limit is always greater than N. Furthermore, for all radii except $\mathcal{R} = 10,000$ m, the downlink is using more resources than the uplink (i.e., $T_u^* < T/2$). We observe also that for $\mathcal{R} = 10,000$ m the problem is infeasible for $S_u \geq 2$; hence, we must resort to SU-MIMO, i.e., $S_u = 1$.

We repeat the same study for the other settings in Table 3.4. To reduce the overall computations, we make the following observations a priori: (i) for the double BS power setting, we may reuse the UL results from the baseline scenario because changing $P_{\max}$ has no impact on the UL user limit (problem $\mathbf{P_u}$ is not dependent on $P_{\max}$); (ii) for the double bandwidth setting, for a given $\mathcal{V}_u = (T_u, S_u)$ we may reuse $n(\mathcal{V}_u, L)$ (the subchannels necessary to achieve MBR_u) from the baseline (from constraint (3.27), the results of $\mathbf{P_u}$ are determined by $|\mathcal{C}_u(\hat{\mathcal{U}})|$ and not by the total subchannels C); then we may use (3.31) to recompute $U_u(\mathcal{V}_u, L)$ with the larger value of C.

We plot the user limits for each setting in Figure 3.5a as a function of the radius. We observe that the user limit can be doubled when the bandwidth B is doubled, when the number of BS antennas M_{BS} is doubled, or when MBR_d and MBR_u are halved. Adding antennas at the BS might be a solution when an operator is limited in the bandwidth it has at its disposal. On the other hand, doubling the BS power $P_{\max}$ alone only provides a marginal increase to the total number of homes that can be given the MBRs. Counter-intuitively, increasing the antennas at the homes adversely affects the number of homes that can receive the MBR for small cell radii and does not improve it for large radii (the reason for this is explained below).

In Figure 3.5b and Figure 3.5c, we plot the group sizes achieving the user limits in the DL and UL, respectively. Note that, in the DL, the baseline, double bandwidth, and half MBR settings achieve their user limits with the same DL group sizes at all radii except $\mathcal{R} = 10,000$; in the UL, the baseline, double bandwidth, and double power settings achieve their limits with the same UL group sizes at all radii. When $M_{\text{BS}} = 128$ and $M_{\text{H}} = 4$ we have $N = 32$ and, hence, we can form larger groups. Indeed, Figures 3.5b and 3.5c show that this setting achieves the DL and UL user limits with larger group sizes than the other settings. On the other hand, when $M_{\text{BS}} = 64$ and $M_{\text{H}} = 8$ then $N = 8$ and fewer homes can be selected together. At the same time, up to 8 streams could be used per home. However, as Figure 3.6a shows for the DL when $T_u = 10$ and 10 suchannels are allocated per group, when U close to N users are selected simultaneously the effective channel of most streams is so poor that PD selects only one or two streams and it is not possible to give all users MBR_d. In particular, if $U = 6$, less than 4 streams are selected. In contrast, for the baseline setting ($M_{\text{H}} = 4$) all 4 streams could be selected when $U = 6$ (Figure 3.6b). Thus, for the same number of subchannels that we could give a group of 6 homes the MBRs in the baseline case, we can only give the MBRs to a smaller group of homes when $M_{\text{H}} = 8$; hence, under this setting, the user limit is less than the baseline and S_d^* and S_u^* are typically smaller as shown in Figures 3.5b and 3.5c, respectively. Note that when $\mathcal{R} = 10,000$ m, for all settings except the one where $M_{\text{BS}} = 128$, the problem is only feasible if we treat the UL as SU-MIMO (i.e., with the UL configuration $S_u = 1$).

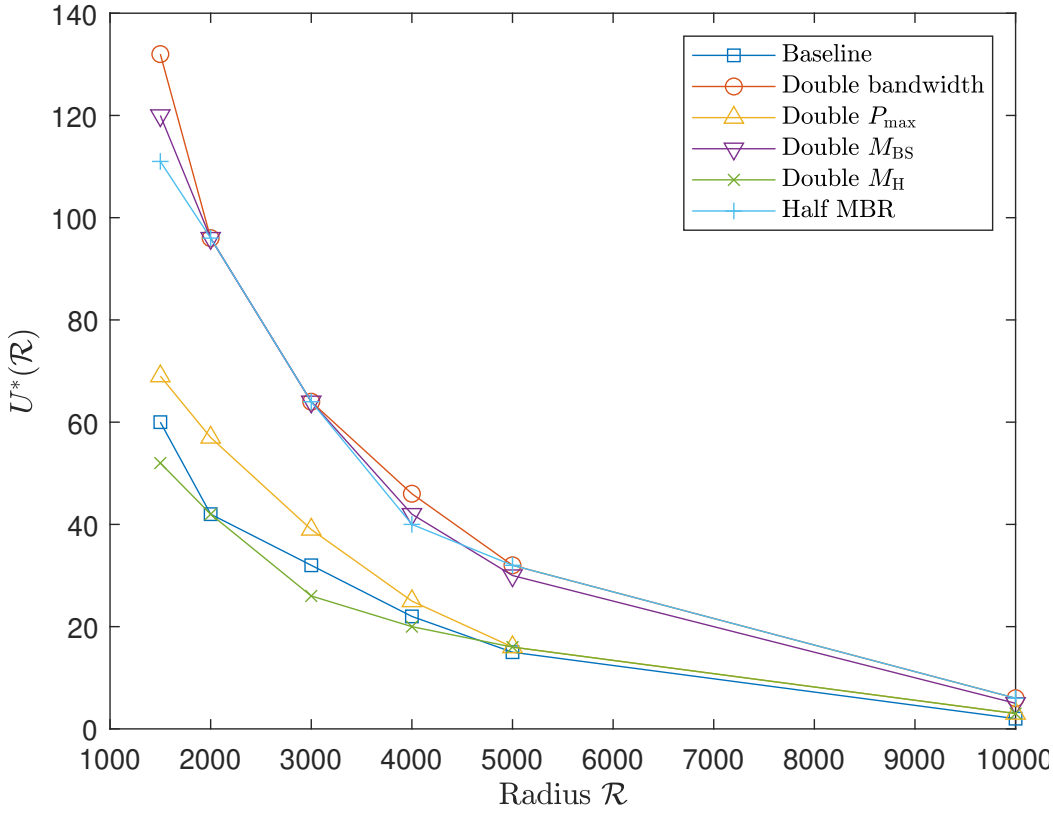

(a) Absolute user limits.

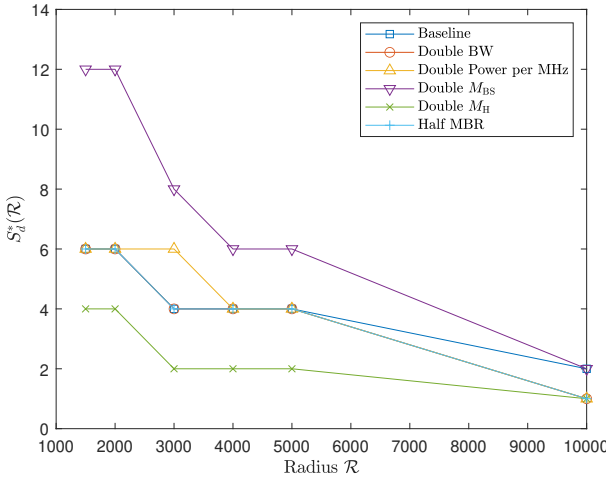

(b) Optimal DL group sizes.

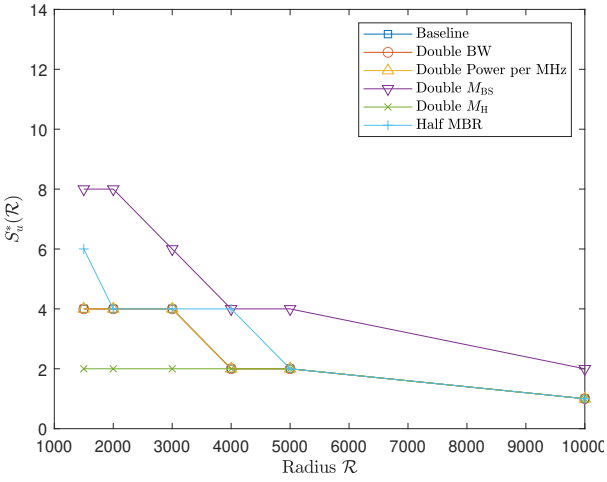

(c) Optimal UL group sizes.

Figure 3.5: Absolute user limits and group sizes required to achieve the limits.

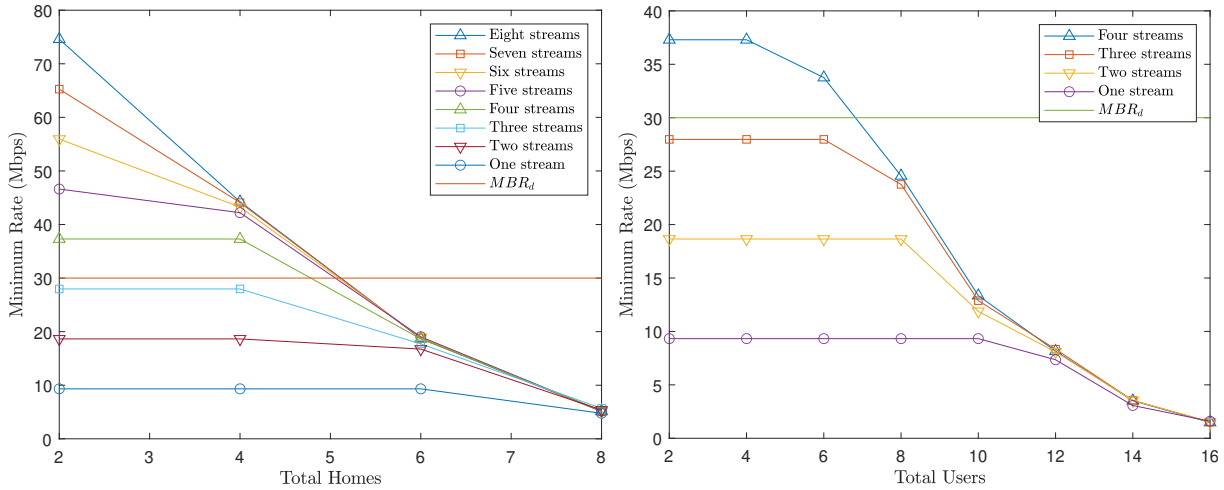

(a) $M_H = 8$, $N = 8$ (b) $M_H = 4$, $N = 16$

Figure 3.6: Minimum DL rates for $U \leq N$ when $M_H = 8$ and $M_H = 4$. For both cases, $\Omega = 100$, $\mathcal{R} = 1500\,\text{m}$, $M_{\text{BS}} = 64$, $P_{\max} = 40\,\text{W}$, $MBR_d = 30\,\text{Mbps}$, $T_u = 10$, and 10 subchannels are allocated to the homes with $P^d_{PRB} = \frac{P_{\max}}{65}$.

3.5.4 Insights for Network Operation

The network planning results provide the user limits (i.e., the maximum number of homes that can be given the MBRs) for different system settings $\mathcal{S}$ as well as the configurations $\mathcal{V}$ necessary to attain those limits. To obtain these results we assumed every home was always active; however, typically, even if an MNO has U^* homes subscribing to its FWA service in a given cell, the number of active homes U would be less than the limit U^* most of the time. The results obtained through the network planning study above can yield information about how the network should be operated when $U < U^*$, i.e., should the configuration remain the same and equal to what we call in the following the "planning configuration" $\mathcal{V}(U^*) = (T_u(U^*), S_d(U^*), S_u(U^*))$ at all times or should it change depending on U?

This question is linked to the following one: if many configurations are U-feasible, which one is the best? This, of course, depends on an additional criteria defining "best". We decided to use the sum-rate (averaged over the 95% realizations that we keep) as that criteria. For example, in Figure 3.7, we show the DL and UL sum-rates that can be attained when $U = 30$ homes are active under the baseline setting and $\mathcal{R} = 1500\,\text{m}$. Each point in the plot corresponds to the U-feasible configuration providing the largest sum-rates on the DL and the UL for a given T_u. From this data it is clear that different configurations

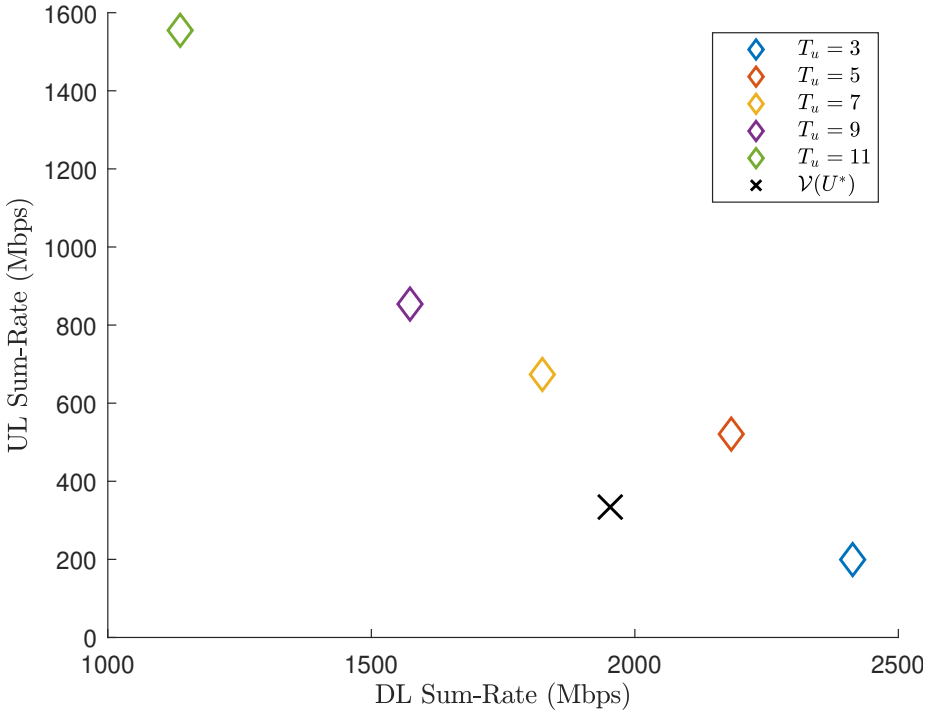

Figure 3.7: Achievable sum-rates for $U = 30$ homes for the baseline setting when $\mathcal{R} = 1500$ m. The rate achieved by the optimal configuration $\mathcal{V}(U^*)$ (where $U^* = 60$) is shown with a $\times$.

can provide different performance on the DL and UL. Moreover, for $U = 30$ there exist U-feasible configurations that can provide better sum-rates than $\mathcal{V}(U^*)$ both on the DL *and* the UL. To determine which configuration is best, we need to decide how much weight the MNO gives to the DL and UL sum-rates. Let α be the DL weight, and define the weighted sum-rate for $U \leq U^*$ and a configuration $\mathcal{V}$ as

$$WSR(\alpha, U, \mathcal{V}) = \alpha \times SR_d(U, \mathcal{V}_d) + (1 - \alpha) \times SR_u(U, \mathcal{V}_u) \tag{3.40}$$

For $U = 30$, the baseline setting and $\mathcal{R} = 1500$ m, if $\alpha = 0.5$ (resp. $\alpha = 0.75$), the best WSR is 1352 Mbps (resp. 1860 Mbps) which is attained with $T_u = 5$ (resp. $T_u = 3$) while if we had used the configuration obtained via planning (i.e., to enable $U^* = 60$), the WSR would have been 1144 Mbps (resp. 1548 Mbps). We found that using a configuration for a number of active homes $U \leq U^*$ could yield performance of up to 30% better than with the planning configuration depending on the values of U, α and the radius among other things.

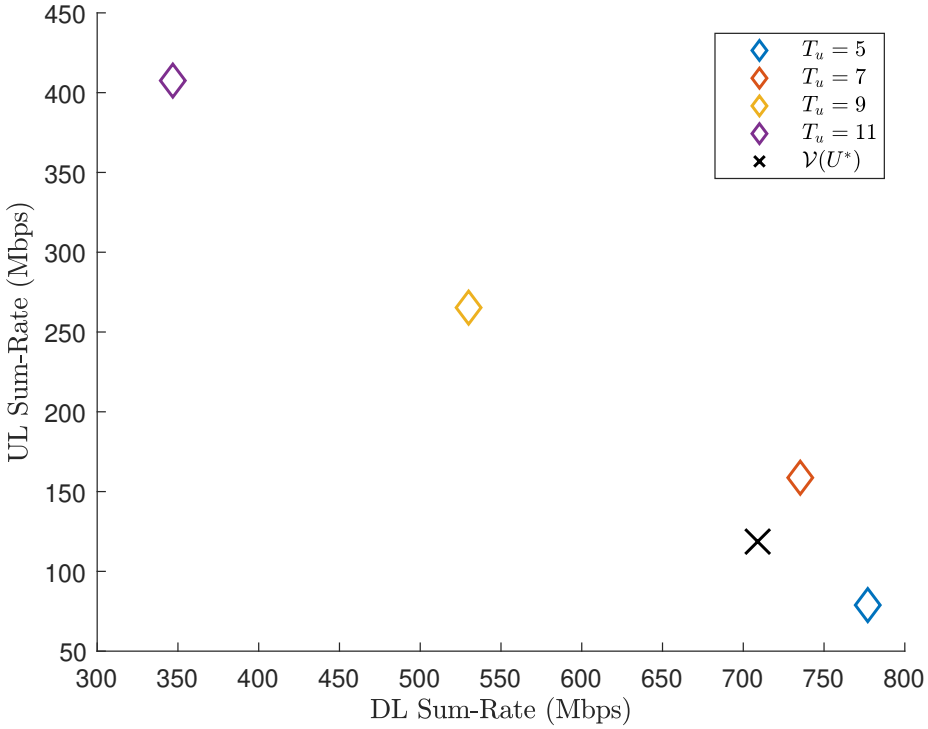

Figure 3.8: Achievable sum-rates for $U = 8$ homes for the baseline setting when $\mathcal{R} = 5000$ m. The rate achieved by the optimal configuration $\mathcal{V}(U^*)$ (where $U^* = 15$) is shown with a $\times$.

We repeat the analysis for the baseline setting for $\mathcal{R} = 5000\,\text{m}$ and $U = 8$ ($U^* = 15$ for this setting and radius) and plot the sum-rates that can be achieved for different T_u in Figure 3.8. In this case there are fewer configurations that are U-feasible, and less configurations that can improve upon $\mathcal{V}(U^*)$ both for the UL and the DL. Indeed, for $\alpha = 0.5$ (resp. $\alpha = 0.75$) the best WSR is 447 Mbps (resp. 603 Mbps), which is attained with $T_u = 7$ (resp. $T_u = 5$), whereas $\mathcal{V}(U^*)$ yields a WSR of 413 Mbps (resp. 561 Mbps). At this radius the performance improvement due to choosing a better configuration for $U \leq U^*$ is limited to 8%.

From these results, we learn that by adapting the configuration to the number of active homes, we might provide noticeable performance improvements to homes, especially if the radius is not too large. In the past, dynamic resource sharing in TDD systems was not practical, and TDD-LTE systems were typically statically or semi-statically configured. However 5G provides significantly more flexibility in this regard, making it possible to

change time-slot configurations frame-to-frame [20]. This flexibility is designed to make it possible for operators to serve diverse, sometimes conflicting user requirements, e.g. DL-heavy eMBB vs. UL-heavy mMTC, but as our work shows, such a scheme could also be used to dynamically operate the network based on the number of active homes. Dynamic TDD could create interference challenges between neighbouring cells and there is ongoing research in this area [21, 22], however this interference should be easier to manage in rural environments.

3.6 Conclusion

In this chapter we have studied the problem of planning a rural 5G-TDD MU-MIMO network operating in the 3.5 GHz band to jointly provide broadband services (and minimum bit rates) in the DL and UL to FWA homes. Since we considered the rural context, we assumed inter-cell interference was low, and thus considered a single cell; furthermore we assumed the environment to have a strong LOS component. We adopted block diagonalization precoding and combining, which eliminates inter-user and inter-stream interference, equal power allocation per subchannel in the DL and in the UL, and a practical MCS function based on 3GPP's 5G NR specification.

We first studied the case where the total number of homes $U \leq N = \left\lceil \frac{M_{\mathrm{BS}}}{M_{\mathrm{H}}} \right\rceil$ (the ratio of antennas at the BS to the antennas at one home) and showed that multi-antenna FWA homes benefit from using multiple data streams. Moreover, we showed that dividing homes into static groups with fixed subchannel allocations ensures many more homes can be given the MBR than selecting close to N homes at the same time. Next we studied the case where $U > N$. Since the system is TDD, determining the maximum number of homes that can be given MBRs jointly in the DL and the UL would require solving the DL and UL problems many times for different numbers of homes U, different group sizes, and different slot configurations. To simplify this process, we developed a procedure to determine the DL and UL user limits for a given time-slot configuration and a given group size. Under this procedure we analyzed the impact of user grouping on the DL and UL user limits for different time-slot configurations and determined the absolute user limits for a number of different system settings at different cell radii. Finally, we provided some insights on how networks can be dynamically operated to provide DL and UL MBRs to FWA homes.

The tools that we have developed and the results that we have obtained can help MNOs decide if introducing FWA for fixed broadband is profitable, i.e., if the user limits are large enough to warrant the implementation of that service. Furthermore, the results can help

MNOs provision their networks to meet a certain user limit.

Chapter 4

Conclusion

4.1 Summary

In this thesis we examined how the rural FB digital divide could be solved by taking advantage of the already high level of cellular coverage in rural communities and deploying 5G FWA to deliver high quality FB services to homes.

In Chapter 2 we provided an overview of the new features in 5G that will be of benefit to solving the FB digital divide, particularly in the FWA context. We reviewed new enhancements that 5G brings to the access, backhaul, network edge and core network. Then we identified a number of open research challenges that remain to be solved so that 5G networks can be appropriately planned and operated to provide robust FWA services in rural communities.

Next, in Chapter 3 we focused on a few of the problems raised from the previous chapter related to planning and operating a rural 5G network to provide MBRs to FWA homes jointly in the DL and UL. In particular, we looked at the case of a single TDD MU-MIMO cell operating in the 3.5 GHz band with a strong LOS component, assuming block diagonalization precoding and combining, equal power allocation per subchannel, and a practical MCS function based on the 5G NR specification. We first studied the problem with a small number of homes to understand the impact of streams and user selection on performance. We learned that (i) homes can benefit from more streams when we select the right number of homes together, and (ii) to give every home the MBRs it is essential to divide them into groups instead of selecting all homes at the same time. Next, we applied our lessons learned about streams and user grouping to study the planning problem with

a large number of homes at different cell radii and with different network settings, such as the bandwidth, power, or number of antennas. Here, our goals were to determine the maximum number of homes that could be given the DL and UL MBRs based on the network settings, and to understand what user group sizes and time-slot configurations were necessary to achieve those limits. We developed a process to more easily determine the user limits based on finding the number of subchannels required to achieve the MBR for a given group size and slot configuration. Lastly, we applied the results learned from the planning study to network operation and showed that the weighted sum-rate of the DL and UL rates given to homes can be improved by up to 30% by dynamically selecting the group sizes and slot-configuration based on the number of homes that are active in the cell.

4.2 Future Research Directions

In Chapter 3 we made a number of assumptions (explicitly or implicitly) to make the problem more tractable. In this section, we discuss how the problem would change if some of those assumptions were relaxed, as well as some potential future research directions.

4.2.1 The Case Where the Backhaul has Limited Capacity

It was implicitly assumed that the backhaul has infinite capacity and is not a limiting factor when planning the cell. If, on the other hand, the backhaul has limited capacity, it could impact how quickly the DL buffers are filled at the BS (due to finite queues elsewhere in the backhaul) and could also limit how quickly UL buffers could be emptied at the homes; hence, even if homes demand the same volume of DL or UL traffic, the possible rates that can be given to each home might differ due to uneven buffer levels. For this reason weighted fair queuing (WFQ) would need to be implemented in the backhaul to fairly distribute traffic among each home's buffer. The WFQ implementation must account for every *cell* sharing a backhaul, so even though BS scheduling is performed per-cell, WFQ must be performed per-backhaul hop, i.e. taking into account homes from possibly many cells at the same time.

To account for the backhaul we can check if the user limit U^* when every user is given the MBRs exceeds the backhaul capacity. Thus if C_d^{bkh} and C_u^{bkh} are the capacities of the backhaul in the DL and the UL directions respectively, then the actual user limit would

be:

$$U^{**} = \min \left\{ U^*, \left\lfloor \frac{C_d^{bck}}{MBR_d} \right\rfloor, \left\lfloor \frac{C_u^{bck}}{MBR_u} \right\rfloor \right\}.$$

In general, MWP2P links are FDD and divide the bandwidth equally between DL and UL [24], but depending on the state of the queues in the network, the instantaneous capacities in each direction could change from frame to frame.

4.2.2 Overhead of CSI for MU-MIMO

To perform BD precoding and combining we assumed that the base station has perfect knowledge of the CSI. CSI estimation is obtained through the transmission of pilot symbols in the UL and DL, which occupy a certain number of OFDM symbols of overhead per frame. Thus, in practice, there is a percentage of the frame dedicated to overhead that cannot be used for data transmission. In MU-MIMO systems orthogonal CSI pilots are required for every active home (i.e., homes have distinct pilots), hence the total CSI overhead scales relative to the number of active homes [65,66]. Hence, as more and more homes are added to a massive MIMO cell the ratio of PRBs used for data transmission will diminish relative to those used for CSI estimation. Thus, the real user limit would be lower than predicted.

CSI pilots are only needed for the homes scheduled in the same coherence block, and in the context of this problem, since homes are fixed the coherence time is expected to be large (several frames or longer). Thus, we expect there to be one coherence block per frame, and hence we may assume that we only need one pilot per home per frame.

4.2.3 User Grouping Strategy

We grouped homes together arbitrarily without consideration of their location or channel. However, smarter user grouping strategies that aim to maximize the effective channel resulting from the precoding and combining process could make it such that more homes could receive the DL and UL MBRs concurrently. If CSI overhead is also considered, smart grouping strategies can further be adopted to reduce overhead by reusing pilots for homes with similar channels [42]. This is particularly applicable if we consider the fact that in practice homes might be distributed in clusters rather than randomly scattered throughout the cell.

4.2.4 Planning the Network for Heterogeneous Services

Operators might offer different MBRs to different homes under different FB packages. To address this, problems $\mathbf{P_d}$ and $\mathbf{P_u}$ would require additional constraints of the form $\lambda_k \geq MBR_{k,d}$ and $\lambda'_k \geq MBR_{k,u}$, which respectively consider the DL and UL MBRs of home k. The difficulty with this assumption is that it prevents us from adopting the simplified approach we used to compute the user limits in this thesis. User limits would then need to be computed using brute force techniques.

We might also consider the presence of mobile users, which are typically provided non-MBR (i.e., best effort) services. If we approached the problem by grouping mobile users with homes, we would have to account for the fact that the mobile users' channels change throughout the frame, hence precoding and combining would need to be performed per-PRB instead of per-subchannel. If instead we determine at the outset that FWA users will only be grouped with FWA users and that they will always receive a certain minimum amount of the bandwidth, then the user limits can be computed as we proposed in Chapter 3.

4.2.5 Impact of mmWave Spectrum

Our study was conducted using a 3.5 GHz mid-band, which we believe is better suited for rural applications than mmWave; however, some authors have suggested that rural FWA services could be provided using mmWave [8, 13, 14]. Although mmWave channels would experience much greater path loss under the cell radii that we considered, it is expected that operators could compensate for this with larger system bandwidths, since there is a much greater availability of mmWave spectrum. Hence, if we were to augment our study to include mmWave we would repeat the analysis with a larger bandwidth and larger number of subchannels. mmWave also uses different NR frame numerologies than mid-bands [7, 18], resulting in wider subchannel bandwidths and shorter slot durations (the frame length is still 10ms; hence, there are more slots in a frame). 3GPP's rural channel model is defined the same for mid-bands and mmWave bands. For mmWave we might also need to consider whether more antennas or higher transmit powers are necessary at the BS or homes. Overall, conducting a similar analysis for mmWave would not change the problem formulation.

Letter of Copyright Permission

Some material in Section 1.1 and Section 2.3.5 were previously published in Proceedings of the IEEE. © 2020 IEEE. Reprinted, with permission, from [28].

In reference to IEEE copyrighted material which is used with permission in this thesis, the IEEE does not endorse any of the University of Waterloo's products or services. Internal or personal use of this material is permitted. If interested in reprinting/republishing IEEE copyrighted material for advertising or promotional purposes or for creating new collective works for resale or redistribution, please go to http://www.ieee.org/publications_standards/publications/rights/rights_link.html to learn how to obtain a License from RightsLink. If applicable, University Microfilms and/or ProQuest Library, or the Archives of Canada may supply single copies of the dissertation.

References

[1] M. Haight, A. Quan-Haase, and B. Corbett, "Revisiting the digital divide in Canada: the impact of demographic factors on access to the internet, level of online activity, and social networking site usage," *Inf., Commun. Soc.*, vol. 17, no. 4, pp. 503–519, Mar. 2014, doi: 10.1080/1369118X.2014.891633.

[2] L. Robinson *et al.*, "Digital inequalities and why they matter," *Inf., Commun. Soc.*, vol. 18, no. 5, pp. 569–582, Mar. 2015, doi: 10.1080/1369118X.2015.1012532.

[3] "Communications Monitoring Report," Canadian Radio-television and Telecommunications Commission (CRTC), Ottawa, ON, Canada, Tech. Rep., Dec. 2020, Accessed: Jul. 15, 2021. [Online]. Available: https://crtc.gc.ca/pubs/cmr2020-en.pdf

[4] "Telecom Regulatory Policy CRTC 2016-496," Canadian Radio-television and Telecommunications Commission (CRTC), Ottawa, ON, Canada, Tech. Rep., Dec. 2016, Accessed: Jul. 15, 2021. [Online]. Available: https://crtc.gc.ca/eng/archive/2016/2016-496.pdf

[5] 3GPP, "LTE; Evolved Universal Terrestrial Radio Access (E-UTRA); User Equipment (UE) radio transmission and reception," 3rd Generation Partnership Project (3GPP), Technical Specification (TS) 36.101, Jan. 2020, version 16.4.0. [Online]. Available: https://portal.3gpp.org/desktopmodules/Specifications/SpecificationDetails.aspx?specificationId=2411

[6] ——, "5G; NR; User Equipment (UE) radio transmission and reception; Part 1: Range 1 Standalone," 3rd Generation Partnership Project (3GPP), Technical Specification (TS) 38.101-1, Jan. 2020, version 16.2.0. [Online]. Available: https://portal.3gpp.org/desktopmodules/Specifications/SpecificationDetails.aspx?specificationId=3283

[7] ——, "5G; NR; User Equipment (UE) radio transmission and reception; Part 2: Range 2 Standalone," 3rd Generation Partnership Project (3GPP), Technical Specification

(TS) 38.101-2, Jan. 2020, version 16.2.0. [Online]. Available: https://portal.3gpp.org/desktopmodules/Specifications/SpecificationDetails.aspx?specificationId=3284

[8] K. Aldubaikhy, W. Wu, N. Zhang, N. Cheng, and X. Shen, "mmWave IEEE 802.11ay for 5G Fixed Wireless Access," *IEEE Wireless Commun. Mag.*, vol. 27, no. 2, pp. 88–95, Apr. 2020, doi: 10.1109/MWC.001.1900174.

[9] F. W. Vook, E. Visotsky, T. A. Thomas, and A. Ghosh, "Performance Characteristics of 5G mmWave Wireless-to-the-Home," in *2016 50th Asilomar Conference on Signals, Systems and Computers*, Pacific Grove, CA, USA, Nov. 2016, pp. 1181–1185, doi: 10.1109/ACSSC.2016.7869558.

[10] A. Brighente, J. Gambini, and S. Tomasin, "Modular Hybrid Beamforming for mmWave Fixed Wireless Access," *IEEE Wireless Commun. Mag.*, vol. 68, no. 8, pp. 5145–5158, Aug. 2020, doi: 10.1109/TCOMM.2020.2992470.

[11] F. Kaltenberger, M. Kountouris, D. Gesbert, and R. Knopp, "On the Trade-Off Between Feedback and Capacity in Measured MU-MIMO Channels," *IEEE Trans. Wireless Commun.*, vol. 8, no. 9, pp. 4866–4875, Sep. 2009, doi: 10.1109/TWC.2009.081670.

[12] L. Liu, R. Chen, S. Geirhofer, K. Sayana, Z. Shi, and Y. Zhou, "Downlink MIMO in LTE-advanced: SU-MIMO vs. MU-MIMO," *IEEE Commun. Mag.*, vol. 50, no. 2, pp. 140–147, Feb. 2012, doi: 10.1109/MCOM.2012.6146493.

[13] O. Kaddoura *et al.*, "Greenfield Design in 5G FWA Networks," *IEEE Commun. Lett.*, vol. 23, no. 12, pp. 2422–2426, Dec. 2019, doi: 10.1109/LCOMM.2019.2939470.

[14] R. Abozariba, E. Davies, M. Broadbent, and N. Race, "Evaluating the Real-World Performance of 5G Fixed Wireless Broadband in Rural Areas," in *2019 IEEE 2nd 5G World Forum (5GWF)*, Dresden, Germany, Sep. 2019, pp. 465–470, doi: 10.1109/5GWF.2019.8911655.

[15] A. Schumacher, R. Merz, and A. Burg, "3.5 GHz Coverage Assessment with a 5G Testbed," in *2019 IEEE 89th Vehicular Technology Conference (VTC2019-Spring)*, Kuala Lumpur, Malaysia, Apr. 2019, pp. 1–6, doi: 10.1109/VTCSpring.2019.8746551.

[16] Coleago Consulting Ltd, "Estimating the mid-band spectrum needs in the 2025-2030 time frame," GSM Association, London, UK, Technical Report, Jul. 2021, Accessed: Jul. 21, 2021. [Online]. Available: https://www.gsma.com/spectrum/wp-content/uploads/2021/07/Estimating-Mid-Band-Spectrum-Needs.pdf

[17] M. Shafi *et al.*, "5G: A Tutorial Overview of Standards, Trials, Challenges, Deployment, and Practice," *IEEE J. Sel. Areas Commun.*, vol. 35, no. 6, pp. 1201–1221, Jun. 2017, doi: 10.1109/JSAC.2017.2692307.

[18] 3GPP, "5G; NR; Physical channels and modulation," 3rd Generation Partnership Project (3GPP), Technical Specification (TS) 38.211, Jul. 2020, version 16.2.0. [Online]. Available: https://portal.3gpp.org/desktopmodules/Specifications/SpecificationDetails.aspx?specificationId=3213

[19] E. G. Larsson, O. Edfors, F. Tufvesson, and T. L. Marzetta, "Massive MIMO for Next Generation Wireless Systems," *IEEE Commun. Mag.*, vol. 52, no. 2, pp. 186–195, Feb. 2014, doi: 10.1109/MCOM.2014.6736761.

[20] 3GPP, "5G; NR; Physical layer procedures for control," 3rd Generation Partnership Project (3GPP), Technical Specification (TS) 38.213, Jul. 2020, version 16.2.0. [Online]. Available: https://portal.3gpp.org/desktopmodules/Specifications/SpecificationDetails.aspx?specificationId=3215

[21] A. K. Gupta *et al.*, "Rate Analysis and Feasibility of Dynamic TDD in 5G Cellular Systems," in *2016 IEEE International Conference on Communications (ICC)*, Kuala Lumpur, Malaysia, May 2016, pp. 1–6, doi: 10.1109/ICC.2016.7511412.

[22] S. Guo, X. Hou, and H. Wang, "Dynamic TDD and Interference Management Towards 5G," in *2018 IEEE Wireless Communications and Networking Conference (WCNC)*, Barcelona, Spain, Apr. 2018, pp. 1–6, doi: 10.1109/WCNC.2018.8377314.

[23] S. Parkvall *et al.*, "5G NR Release 16: Start of the 5G Evolution," *IEEE Commun. Standards Mag.*, vol. 4, no. 4, pp. 56–63, Dec. 2020, doi: 10.1109/MCOM-STD.011.1900018.

[24] X. Huang, Y. J. Guo, A. Zhang, and V. Dyadyuk, "A Multi-Gigabit Microwave Backhaul," *IEEE Commun. Mag.*, vol. 50, no. 3, pp. 122–129, Mar. 2012, doi: 10.1109/MCOM.2012.6163591.

[25] M. Polese *et al.*, "Integrated Access and Backhaul in 5G mmWave Networks: Potential and Challenges," *IEEE Commun. Mag.*, vol. 58, no. 3, pp. 62–68, Mar. 2020, doi: 10.1109/MCOM.001.1900346.

[26] V. Nguyen, A. Brunstrom, K. Grinnemo, and J. Taheri, "SDN/NFV-Based Mobile Packet Core Network Architectures: A Survey," *IEEE Commun. Surveys & Tutorials*, vol. 19, no. 3, pp. 1567–1602, 3rd Quart. 2017, doi: 10.1109/COMST.2017.2690823.

[27] T. Taleb, K. Samdanis, B. Mada, H. Flinck, S. Dutta, and D. Sabella, "On Multi-Access Edge Computing: A Survey of the Emerging 5G Network Edge Cloud Architecture and Orchestration," *IEEE Commun. Surveys & Tutorials*, vol. 19, no. 3, pp. 1657–1681, 3rd Quart. 2017, doi: 10.1109/COMST.2017.2705720.

[28] A. Lappalainen and C. Rosenberg, "Bridging the Digital Divide: Success Depends on Content Provider and Application Developer Involvement," *Proc. IEEE*, vol. 109, no. 1, pp. 2–10, Jan. 2021, doi: 10.1109/JPROC.2020.3028611.

[29] S. Ferlin-Oliveira, T. Dreibholz, and Ö. Alay, "Tackling the Challenge of Bufferbloat in Multi-Path Transport over Heterogeneous Wireless Networks," in *Proc. 22nd IEEE IWQoS*, May 2014, pp. 123–128, doi: 10.1109/IWQoS.2014.6914310.

[30] Q. De Coninck and O. Bonaventure, "Multipath QUIC: Design and Evaluation," in *Proc. 13th ACM CoNEXT*, Nov. 2017, pp. 160–166, doi: 10.1145/3143361.3143370.

[31] M. Kosek, T. Shreedhar, and V. Bajpai, "Beyond QUIC v1: A First Look at Recent Transport Layer IETF Standardization Efforts," *IEEE Commun. Mag.*, vol. 59, no. 4, pp. 24–29, Apr. 2021, doi: 10.1109/MCOM.001.2000877.

[32] M. Condoluci *et al.*, "Fixed-Mobile Convergence in the 5G Era: From Hybrid Access to Converged Core," *IEEE Netw.*, vol. 33, no. 2, pp. 138–145, Mar./Apr. 2019, doi: 10.1109/MNET.2018.1700462.

[33] K. Samdanis, X. Costa-Perez, and V. Sciancalepore, "From Network Sharing to Multi-Tenancy: The 5G Network Slice Broker," *IEEE Commun. Mag.*, vol. 54, no. 7, pp. 32–39, Jul. 2016, doi: 10.1109/MCOM.2016.7514161.

[34] Innovation, Science and Economic Development Canada, "National Broadband Internet Service Availability Map," Aug. 2020, Accessed: Sep. 1, 2020. [Online]. Available: https://www.ic.gc.ca/app/sitt/bbmap/hm.html?lang=eng

[35] Z. Shen, R. Chen, J. Andrews, R. Heath, and B. Evans, "Low Complexity User Selection Algorithms for Multiuser MIMO Systems With Block Diagonalization," *IEEE Trans. Signal Process.*, vol. 54, no. 9, pp. 3658–3663, Sep. 2006, doi: 10.1109/TSP.2006.879269.

[36] M. Jaber, Z. Dawy, N. Akl, and E. Yaacoub, "Tutorial on LTE/LTE-A Cellular Network Dimensioning Using Iterative Statistical Analysis," *IEEE Commun. Surveys & Tutorials*, vol. 18, no. 2, pp. 1355–1383, 2nd Quart. 2016, doi: 10.1109/COMST.2015.2513440.

[37] A. Taufique, M. Jaber, A. Imran, Z. Dawy, and E. Yacoub, "Planning Wireless Cellular Networks of Future: Outlook, Challenges and Opportunities," *IEEE Access*, vol. 5, pp. 4821–4845, 2017, doi: 10.1109/ACCESS.2017.2680318.

[38] L. Chiaraviglio, C. Di Paolo, and N. Blefari Melazzi, "5G Network Planning under Service and EMF Constraints: Formulation and Solutions," *IEEE Trans. Mobile Comput.*, pp. 1–25, 2021, doi: 10.1109/TMC.2021.3054482.

[39] M. U. Khan, A. García-Armada, and J. J. Escudero-Garzás, "Service-Based Network Dimensioning for 5G Networks Assisted by Real Data," *IEEE Access*, vol. 8, pp. 129 193–129 212, 2020, doi: 10.1109/ACCESS.2020.3009127.

[40] M. Kashef, M. Ismail, E. Serpedin, and K. Qaraqe, "Balanced Dynamic Planning in Green Heterogeneous Cellular Networks," *IEEE J. Sel. Areas Commun.*, vol. 34, no. 12, pp. 3299–3312, Dec. 2016, doi: 10.1109/JSAC.2016.2624098.

[41] H. Ghazzai, E. Yaacoub, M.-S. Alouini, Z. Dawy, and A. Abu-Dayya, "Optimized LTE Cell Planning With Varying Spatial and Temporal User Densities," *IEEE Trans. Veh. Technol.*, vol. 65, no. 3, pp. 1575–1589, Mar. 2016, doi: 10.1109/TVT.2015.2411579.

[42] E. Castañeda, A. Silva, A. Gameiro, and M. Kountouris, "An Overview on Resource Allocation Techniques for Multi-User MIMO Systems," *IEEE Commun. Surveys & Tutorials*, vol. 19, no. 1, pp. 239–284, 1st Quart. 2017, doi: 10.1109/COMST.2016.2618870.

[43] A. Colpaert, E. Vinogradov, and S. Pollin, "Fixed mmWave Multi-User MIMO: Performance Analysis and Proof-of-Concept Architecture," in *2020 IEEE 91st Vehicular Technology Conference (VTC2020-Spring)*, Antwerp, Belgium, May 2020, pp. 1–5, doi: 10.1109/VTC2020-Spring48590.2020.9128958.

[44] Q. Spencer, A. Swindlehurst, and M. Haardt, "Zero-Forcing Methods for Downlink Spatial Multiplexing in Multiuser MIMO Channels," *IEEE Trans. Signal Process.*, vol. 52, no. 2, pp. 461–471, Feb. 2004, doi: 10.1109/TSP.2003.821107.

[45] C.-B. Chae, S. Shim, and R. W. Heath, "Block Diagonalized Vector Perturbation for Multiuser MIMO Systems," *IEEE Trans. Wireless Commun.*, vol. 7, no. 11, pp. 4051–4057, Nov. 2008, doi: 10.1109/T-WC.2008.070262.

[46] K. Zu, R. C. de Lamare, and M. Haardt, "Generalized Design of Low-Complexity Block Diagonalization Type Precoding Algorithms for Multiuser MIMO Systems,"

IEEE Wireless Commun. Mag., vol. 61, no. 10, pp. 4232–4242, Oct. 2013, doi: 10.1109/TCOMM.2013.090513.130038.

[47] D. W. K. Ng and R. Schober, "Energy-Efficient Resource Allocation in OFDMA Systems with Large Numbers of Base Station Antennas," in *2012 IEEE International Conference on Communications (ICC)*, Ottawa, ON, Canada, Jun. 2012, pp. 5916–5920, doi: 10.1109/ICC.2012.6364677.

[48] F. R. M. Lima, T. F. Maciel, W. C. Freitas, and F. R. P. Cavalcanti, "Improved Spectral Efficiency With Acceptable Service Provision in Multiuser MIMO Scenarios," *IEEE Trans. Veh. Technol.*, vol. 63, no. 6, pp. 2697–2711, Jul. 2014, doi: 10.1109/TVT.2013.2293333.

[49] A. Zappone, L. Sanguinetti, G. Bacci, E. Jorswieck, and M. Debbah, "Distributed Energy-Efficient UL Power Control in Massive MIMO with Hardware Impairments and Imperfect CSI," in *2015 International Symposium on Wireless Communication Systems (ISWCS)*, Brussels, Belgium, Aug. 2015, pp. 311–315, doi: 10.1109/ISWCS.2015.7454353.

[50] A. Zappone, L. Sanguinetti, G. Bacci, E. Jorswieck, and M. Debbah, "Energy-Efficient Power Control: A Look at 5G Wireless Technologies," *IEEE Trans. Signal Process.*, vol. 64, no. 7, pp. 1668–1683, Apr. 2016, doi: 10.1109/TSP.2015.2500200.

[51] W. W. L. Ho and Y.-C. Liang, "Optimal Resource Allocation for Multiuser MIMO-OFDM Systems With User Rate Constraints," *IEEE Trans. Veh. Technol.*, vol. 58, no. 3, pp. 1190–1203, Mar. 2009, doi: 10.1109/TVT.2008.927721.

[52] T. Yoo and A. Goldsmith, "On the Optimality of Multiantenna Broadcast Scheduling Using Zero-Forcing Beamforming," *IEEE J. Sel. Areas Commun.*, vol. 24, no. 3, pp. 528–541, Mar. 2006, doi: 10.1109/JSAC.2005.862421.

[53] A. M. El Hajj and Z. Dawy, "Dynamic Joint Switching Point Configuration and Resource Allocation in TDD-OFDMA Wireless Networks," in *2011 IEEE Global Telecommunications Conference - GLOBECOM 2011*, Houston, TX, USA, Dec. 2011, pp. 1–6, doi: 10.1109/GLOCOM.2011.6133553.

[54] N. Zorba and C. Verikoukis, "Energy Optimization for Bidirectional Multimedia Communication in Unsynchronized TDD Systems," *IEEE Syst. J.*, vol. 10, no. 2, pp. 797–804, Jun. 2016, doi: 10.1109/JSYST.2015.2456072.

[55] Y. Zhang, P. Mitran, and C. Rosenberg, "Joint Resource Allocation for Linear Precoding in Downlink Massive MIMO Systems," *IEEE Wireless Commun. Mag.*, vol. 69, no. 5, pp. 3039–3053, May 2021, doi: 10.1109/TCOMM.2021.3053040.

[56] 3GPP, "5G; Study on channel model for frequencies from 0.5 to 100 GHz," 3rd Generation Partnership Project (3GPP), Technical Report (TR) 38.901, Jan. 2020, version 16.1.0. [Online]. Available: https://portal.3gpp.org/desktopmodules/Specifications/SpecificationDetails.aspx?specificationId=3173

[57] J. Liu, "Be Cautious When Using the FIR Channel Model With the OFDM-Based Communication Systems," *IEEE Trans. Veh. Technol.*, vol. 58, no. 3, pp. 1607–1612, Mar. 2009, doi: 10.1109/TVT.2008.928897.

[58] D. Ying, F. W. Vook, T. A. Thomas, D. J. Love, and A. Ghosh, "Kronecker product correlation model and limited feedback codebook design in a 3D channel model," in *2014 IEEE International Conference on Communications (ICC)*, Sydney, NSW, Australia, Jun. 2014, pp. 5865–5870, doi: 10.1109/ICC.2014.6884258.

[59] H. Lim, Y. Jang, and D. Yoon, "Bounds for Eigenvalues of Spatial Correlation Matrices With the Exponential Model in MIMO Systems," *IEEE Trans. Wireless Commun.*, vol. 16, no. 2, pp. 1196–1204, Feb. 2017, doi: 10.1109/TWC.2016.2641419.

[60] L. Fan, Y. Li, and M. Zhao, "Dual-polarized very large antenna array with exponential correlation matrix," in *2013 IEEE 24th Annual International Symposium on Personal, Indoor, and Mobile Radio Communications (PIMRC)*, London, UK, Sep. 2013, pp. 1386–1391, doi: 10.1109/PIMRC.2013.6666357.

[61] 3GPP, "5G; NR; Physical layer procedures for data," 3rd Generation Partnership Project (3GPP), Technical Specification (TS) 38.214, Jul. 2020, version 16.2.0. [Online]. Available: https://portal.3gpp.org/desktopmodules/Specifications/SpecificationDetails.aspx?specificationId=3216

[62] S. Lagen, K. Wanuga, H. Elkotby, S. Goyal, N. Patriciello, and L. Giupponi, "New Radio Physical Layer Abstraction for System-Level Simulations of 5G Networks," in *ICC 2020 - 2020 IEEE International Conference on Communications (ICC)*, Dublin, Ireland, Jun. 2020, pp. 1–7, doi: 10.1109/ICC40277.2020.9149444.

[63] J. C. Ikuno, M. Wrulich, and M. Rupp, "System Level Simulation of LTE Networks," in *2010 IEEE 71st Vehicular Technology Conference*, Taipei, Taiwan, May 2010, pp. 1–5, doi: 10.1109/VETECS.2010.5494007.

[64] D. López-Pérez, Á. Ladányi, A. Jüttner, H. Rivano, and J. Zhang, "Optimization method for the joint allocation of modulation schemes, coding rates, resource blocks and power in self-organizing LTE networks," in *2011 Proceedings IEEE INFOCOM*, Shanghai, China, Apr. 2011, pp. 111–115, doi: 10.1109/INFCOM.2011.5934888.

[65] H. Q. Ngo, E. G. Larsson, and T. L. Marzetta, "Massive MU-MIMO Downlink TDD Systems with Linear Precoding and Downlink Pilots," in *2013 51st Annual Allerton Conference on Communication, Control, and Computing (Allerton)*, Monticcello, IL, Oct. 2013, pp. 293–298, doi: 10.1109/Allerton.2013.6736537.

[66] M. Karlsson and E. G. Larsson, "On the Operation of Massive MIMO with and without Transmitter CSI," in *2014 IEEE 15th International Workshop on Signal Processing Advances in Wireless Communications (SPAWC)*, Toronto, ON, Jun. 2014, pp. 1–5, doi: 10.1109/SPAWC.2014.6941305.